LI
LABORATORY INVESTIGATION
THE BASIC AND TRANSLATIONAL PATHOLOGY RESEARCH JOURNAL
VOLUME 100 | SUPPLEMENT 1 | MARCH 2020

ABSTRACTS

NEUROPATHOLOGY AND OPHTHALMIC PATHOLOGY (1697-1738)

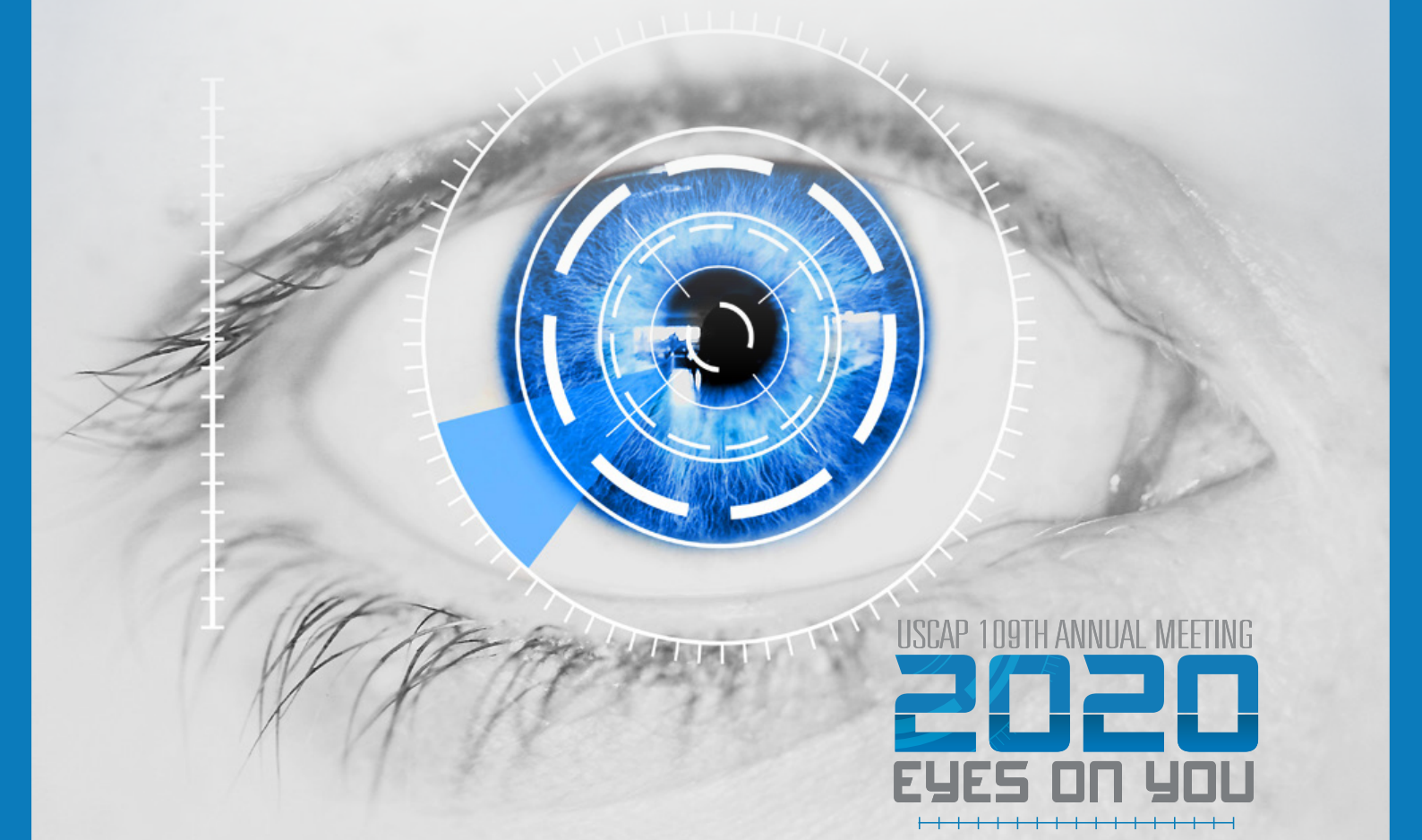

FEBRUARY 29-MARCH 5, 2020

LOS ANGELES CONVENTION CENTER
LOS ANGELES, CALIFORNIA

Published by
SPRINGER NATURE
www.ModernPathology.org

USCAP
Creating a Better Pathologist
AN OFFICIAL JOURNAL OF THE UNITED STATES AND CANADIAN ACADEMY OF PATHOLOGY

EDUCATION COMMITTEE

Jason L. Hornick, Chair

Rhonda K. Yantiss, Chair, Abstract Review Board and Assignment Committee

Laura W. Lamps, Chair, CME Subcommittee

Steven D. Billings, Interactive Microscopy Subcommittee

Raja R. Seethala, Short Course Coordinator

Ilan Weinreb, Subcommittee for Unique Live Course Offerings

David B. Kaminsky (Ex-Officio)

Zubair Baloch
Daniel Brat
Ashley M. Cimino-Mathews
James R. Cook
Sarah Dry
William C. Faquin
Yuri Fedoriw
Karen Fritchie
Lakshmi Priya Kunju
Anna Marie Mulligan
Rish K. Pai
David Papke, Pathologist-in-Training
Vinita Parkash
Carlos Parra-Herran
Anil V. Parwani
Rajiv M. Patel
Deepa T. Patil
Lynette M. Sholl
Nicholas A. Zoumberos, Pathologist-in-Training

ABSTRACT REVIEW BOARD

Benjamin Adam
Narasimhan Agaram
Rouba Ali-Fehmi
Ghassan Allo
Isabel Alvarado-Cabrero
Catalina Amador
Roberto Barrios
Rohit Bhargava
Jennifer Boland
Alain Borczuk
Elena Brachtel
Marilyn Bui
Eric Burks
Shelley Caltharp
Barbara Centeno
Joanna Chan
Jennifer Chapman
Hui Chen
Beth Clark
James Conner
Alejandro Contreras
Claudiu Cotta
Jennifer Cotter
Sonika Dahiya
Farbod Darvishian
Jessica Davis
Heather Dawson
Elizabeth Demicco
Katie Dennis
Anand Dighe
Suzanne Dintzis
Michelle Downes
Andrew Evans
Michael Feely
Dennis Firchau
Gregory Fishbein
Andrew Folpe
Larissa Furtado
Billie Fyfe-Kirschner
Giovanna Giannico
Anthony Gill
Paula Ginter
Tamara Giorgadze
Purva Gopal
Anuradha Gopalan
Abha Goyal
Rondell Graham
Alejandro Gru
Nilesh Gupta
Mamta Gupta
Gillian Hale
Suntrea Hammer
Malini Harigopal
Douglas Hartman
John Higgins
Mai Hoang
Mojgan Hosseini
Aaron Huber
Peter Illei
Doina Ivan
Wei Jiang
Vickie Jo
Kirk Jones
Neerja Kambham
Chiah Sui Kao
Dipti Karamchandani
Darcy Kerr
Ashraf Khan
Francesca Khani
Rebecca King
Veronica Klepeis
Gregor Krings
Asangi Kumarapeli
Alvaro Laga
Steven Lagana
Keith Lai
Michael Lee
Cheng-Han Lee
Madelyn Lew
Zaibo Li
Faqian Li
Ying Li
Haiyan Liu
Xiuli Liu
Yen-Chun Liu
Lesley Lomo
Tamara Lotan
Anthony Magliocco
Kruti Maniar
Emily Mason
David McClintock
Bruce McManus
David Meredith
Anne Mills
Neda Moatamed
Sara Monaco
Atis Muehlenbachs
Bita Naini
Dianna Ng
Tony Ng
Michiya Nishino
Scott Owens
Jacqueline Parai
Yan Peng
Manju Prasad
Peter Pytel
Stephen Raab
Joseph Rabban
Stanley Radio
Emad Rakha
Preetha Ramalingam
Priya Rao
Robyn Reed
Michelle Reid
Natasha Rekhtman
Jordan Reynolds
Michael Rivera
Andres Roma
Avi Rosenberg
Esther Rossi
Peter Sadow
Steven Salvatore
Souzan Sanati
Anjali Saqi
Jeanne Shen
Jiaqi Shi
Gabriel Sica
Alexa Siddon
Deepika Sirohi
Kalliopi Siziopikou
Sara Szabo
Julie Teruya-Feldstein
Khin Thway
Rashmi Tondon
Jose Torrealba
Andrew Turk
Evi Vakiani
Christopher VandenBussche
Paul VanderLaan
Olga Weinberg
Sara Wobker
Shaofeng Yan
Anjana Yeldandi
Akihiko Yoshida
Gloria Young
Minghao Zhong
Yaolin Zhou
Hongfa Zhu
Debra Zynger

To cite abstracts in this publication, please use the following format: **Author A, Author B, Author C, et al. Abstract title (abs#). In "File Title."** ***Laboratory Investigation*** **2020; 100 (suppl 1): page#**

1697 Clinical Validation of Digital Imaging System for Remote Frozen Sections in Neuropathology

Nfn Aakash[1], Mei Lin[2], Meenakshi Bhattacharjee[3], Leomar Ballester[4]
[1]The University of Texas Health Science Center at Houston, Houston, TX, [2]UT Health Science Center at Houston, Houston, TX, [3]University of Texas Houston, Houston, TX, [4]UTHealth McGovern Medical School, Houston, TX

Disclosures: Nfn Aakash: None; Mei Lin: None; Meenakshi Bhattacharjee: None

Background: The use of high-resolution digital imaging currently had been increasingly implemented in pathology. Validation of imaging tools, including cameras, computers, scanners, and digital management systems have been reviewed by the College of American Pathologists (CAP). The current guidelines are as follows:

1. Validation should be appropriate for and applicable to intended clinical use
2. Emulate real world clinical environment
3. Requires at least 60 cases for one application
    a. Must include another 20 cases for each additional sub-application
4. Establish intra observer diagnostic concordance between digital and glass slides
5. Significant changes to whole slide imaging (WSI) requires revalidation

Here we describe the validation of the digital imaging system model for frozen tissue diagnosis by Neuropathology at University of Texas at Houston.

Design: 60 consecutive central nervous system cases with frozen tissue diagnosis were selected from the archives. Frozen call scenarios were constructed for each case. Adequate history was provided to the off-site pathologists. Digital imaging system including a microscope (Olympus BX41) with attached camera (Olympus DP26-CU) were used by a pathology resident to review slides. A board certified neuropathologist used an iMac retina 5K 27-inch display to view the slides on real time using the intranet system and render a frozen tissue diagnosis. Results and time to final frozen diagnosis were compared for concordance with the previous light microscopy glass slide diagnoses.

Results: Results and time to final diagnosis were compared between the digital imaging and light microscopy. Concordance for the frozen tissue diagnoses was 58/60 (96%). Reasons for discordance included faint staining or partially damaged glass slide. Mean time to final diagnosis was 4.4 minutes.

Figure 1 - 1697

Conclusions: We achieved highly satisfactory diagnostic concordance between digital and glass slide intra operative diagnoses. Authors conclude that discordance can be avoided by proper slide handling, and staining. Improved ergonomics training to minimize computer fatigue is also recommended.

1698 PlexinA1 Receptor and its Ligand, Axon Guidance Molecule Semaphorin 6D are Implicated in Medulloblastoma Progression

Mohammed Alshemeili[1], David Meyronet[2]
[1]Lyon, Rhone Alpe, France, [2]Centre de Pathologie et Neuropathologie Est, Bronx, Rhone Alpe, France

Disclosures: Mohammed Alshemeili: None

Background: Medulloblastomas (MBs) are a heterogeneous group of cerebellum embryonic tumors. All Desmoplastic and some classic MBs, belong to SHH subgroup, one of the 4 recently defined molecular subgroups. Molecular studies suggested that axonal guidance molecules were specifically involved in SHH and 4th subgroups of MBs. However their contribution to tumor progression is poorly understood. Interestingly, (Sema6D)/Plexin-A1 has been identified as a pro-migratory pathway in cardiac precursor cells and mesothelioma cells. Our aim was to determine expression and role of Sema6D/Plexin-A1 pathway among MBs.

Design: Desmoplastic MBs (DAOY) and classic MBs (DEV) cells were compared in vitro. The influence of Sema6D/PlexinA1 activation on migration was assessed using Sema6D stimulation and plexinA1 overexpression. A translational study compared PlexinA1 transcripts and protein expression among MBs subgroups and to metastatic status.

Results: PlexinA1 protein expression paralleled mRNA levels and bound Sema6D in human PlexinA1 positive MBs. Interestingly, transfection of PLEXINA1 in negative DAOY cells led to a 2 fold increased migration under Sema6D stimulation while transfection of PLEXINA1 truncated forms missing Sema domain led to the opposite effect. Transcriptomic analysis on human MB samples demonstrated that PlexinA1 mRNA expression wasn't significantly different in classic compared to desmoplastic MBs. Interestingly, PlexinA1 expression was higher in metastatic patients than in M0-MBs.

Our data suggest a specific involvement of Sema6D/Plexin-A1 pathway in MB cells migration. It is potentially involved in the molecular subgroup 4 of MBs. Its promigratory effect may participate to the metastatic process of this subset of MBs

Figure 1 - 1698

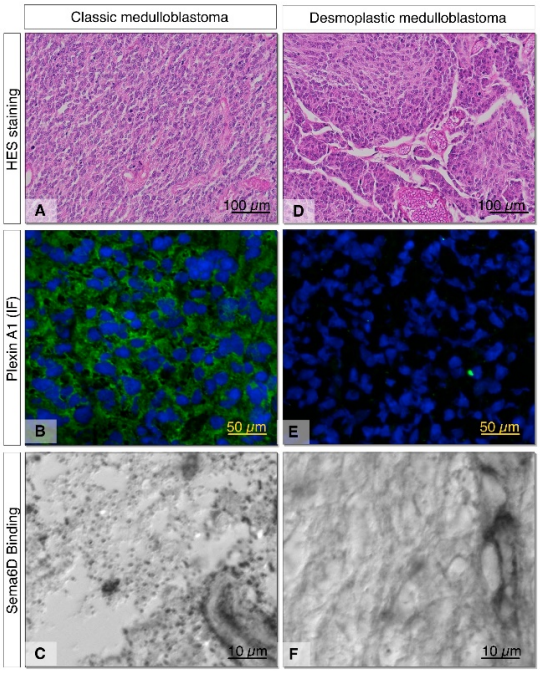

Figure 2 - 1698

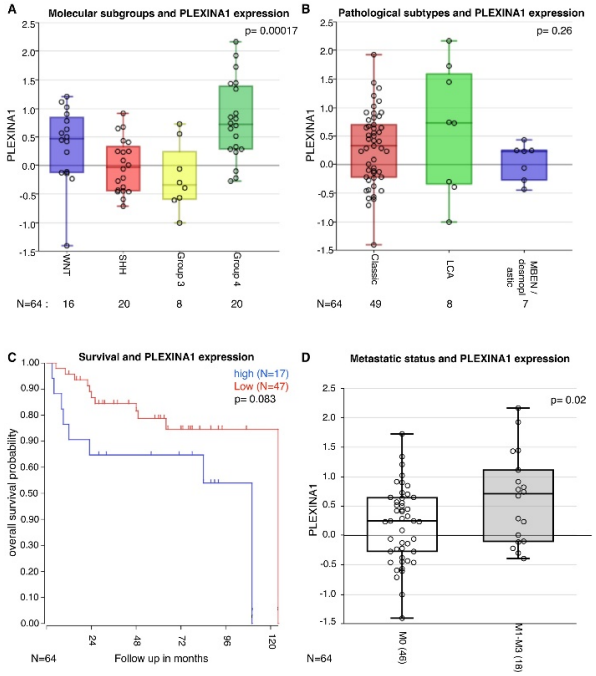

Conclusions: To sum up, we underscored a new role for Sema6D/PlexinA1, promoting MB cell migration and further correlated PlexinA1 expression to metastatic status. Altogether these data showed that Sema6D/Plexin-A1 may provide new insights into MB metastatic potential. The striking in vitro blockade of cell migration resulting from PlexinA1 ectodomain deletion let envision new fields of research to target this receptor in MBs.

1699 PD-L1 (22C3) Expression in Primary and Recurrent Glioblastoma

Leonidas Arvanitis[1], Hsiao-Wei Chen[2], Carrie Louie[2], Massimo D'Apuzzo[3], Dongqing Gu[2], Hooi Yew[3], Jana Portnow[2], Benham Badie[2], Raju Pillai[2], Patricia Aoun[2], Milhan Telatar[2], Michelle Afkhami[2]
[1]City of Hope National Medical Center, Los Angeles, CA, [2]City of Hope National Medical Center, Duarte, CA, [3]City of Hope, Duarte, CA

Disclosures: Leonidas Arvanitis: None; Hsiao-Wei Chen: None; Carrie Louie: None; Hooi Yew: None; Raju Pillai: None; Milhan Telatar: None; Michelle Afkhami: None

Background: The programmed cell death 1 (PD-1) pathway is a recently recognized mechanism of tumor immune evasion. In this study, programmed cell death ligand 1 (PD-L1) expression was evaluated in 66 patients with diagnosed glioblastoma (GBM): 41 primary GBM and 25 recurrent GBM cases. We aimed to evaluate the pattern of expression of PD-L1 (22C3) by immunohistochemistry and assess its relationship with the common molecular prognostic and predictive markers.

Design: Retrospective study of cases sent for HopeSeq Glioma from December 2017 to August 2019. PD-L1 clone 22C3 and MGMT testing performed on all the GBM samples from the same time period. For HopeSeq Glioma assay, nucleic acids was extracted to perform targeted next-generation sequencing by Ion AmpliSeqtm technology and analyzed with the Ion Reporter and NextGENe softwares. PD-L1 protein expression is defined by using Tumor Proportion Score (TPS) and are classified in three groups: 1. PD-L1 with high expression if scored as >=50%, expression if scored = 1-49% and no expression if scored as <1%. We used Fisher Exact Test to compare the PD-L1 groups with the cases with *NF1, RB1, PTEN, IDH1, EGFR, EGFR vIII, TERT, TP53, PIK3CA, ATRX* mutations detected by HopeSeq glioma assay.

Results: Among our 66 GBM cases, [primary = 41 (62%), recurrent = 25 (38%)], PD-L1 expression was absent in 43% of primary GBM cases and 16% of recurrent GBM cases. PD-L1 showed expression in 44% of primary GBM and 60% of recurrent GBM cases and showed high expression in 12% of primary and 24% in recurrent cases. A summary of PD-L1 expression and its relationship with the common molecular prognostic and predictive markers are shown in table 1.

Mutation	High Expression (n=11)	Expressed (n=33)	No expression (n=22)
IDH-WT	11	31	18
IDH-mut	0	2	4
TP53-mut	4	14	12
NF1-mut	4	9	0
EGFR-mut	2	5	3
PTEN-mut	1	10	5
PIK3CA-mut	4	2	3
TERT-mut	9	26	14
ATRX-mut	0	2	5
RB1-mut	2	3	3
PDGFRA amplification	0	5	5
EGFR amplification	3	10	6
EGFR viii-mut	2	5	2
MGMT	2	17	10

Conclusions: This study shows that PD-L1 (22C3) can be variably expressed in both primary and recurrent glioblastoma. PD-L1 (22C3) positive immunoreactivity in 66 cases of GBM can be a useful marker for future clinical trials and may implicate a potentially effective therapeutic target in this highly aggressive type of primary CNS malignancy.

1700 Peculiarities of Non-Neuroendocrine Tumors of the Posterior Pituitary Gland: Case Series from a Referral Pituitary Centre

Sofia Asioli[1], Doriana Donatella Di Nanni[2], Angelo Corradini[3], Francesca Ambrosi[4], Diego Mazzatenta[5], Matteo Zoli[5], Marco Faustini-Fustini[5], Federica Guaraldi[5], Federico Roncaroli[6]
[1]University of Bologna, Bologna, Italy, [2]S.Orsola-Malpighi Hospital, University of Bologna, Bologna, Italy, [3]Pathology Unit, S.Orsola-Malpighi Hospital, University of Bologna, Bologna, Italy, [4]S.Orsola-Malpighi Hospital, University of Bologna, Bari, Italy, [5]IRCCS Istituto delle Scienze Neurologiche di Bologna, Bologna, Italy, [6]Division of Neuroscience and Experimental Psychology Faculty of Medicine, Manchester, Manchester, United Kingdom

Disclosures: Sofia Asioli: None; Doriana Donatella Di Nanni: None; Angelo Corradini: None; Francesca Ambrosi: None; Diego Mazzatenta: None; Matteo Zoli: None; Marco Faustini-Fustini: None; Federica Guaraldi: None; Federico Roncaroli: None

Background: Non-neuroendocrine tumors of the posterior pituitary gland (NNET-PPG), i.e. pituicytoma (PO), granular cell tumor (GST) and spindle cell oncocytoma (SCO) are rare. According to 2017 WHO classification they belong to the same family of lesions.

Despite being considered benign, SCO can have a worse outcome. Aim of this study is to report typical clinic-pathological features, management and outcome of our series of NNET-PPG to guide their diagnosis and treatment.

Design: Posterior pituitary lesions operated between 2007 and 2018 at a referral Pituitary Center, were reviewed by four pathologists. Cases with available clinical, radiological, histopathological and follow-up data were included. Immunohistochemical evaluation of antibodies S100, GFAP, TTF1, Ki67 were performed to confirm the diagnosis.

Results: Thirteen (5 females and 8 males) NNET-PPG were collected. Mean age at surgery was 48.5 years (range 26-77 years). The most frequent signs at diagnosis were hyperprolactinemia and diabetes insipidus, often associated with hypopituitarism. Two cases were located in the suprasellar region while the remaining cases are intrasellar. No invasive lesion was detected. Complete surgical excision was obtained in all but one patient. Six cases were diagnosed as PO, five as SCO and 2 as GCT. All tumors expressed TTF-1; S-100 was positive in 11and GFAP in 5. Mitoses were less than 1x10 HPF in PO and 2x10 in SCO; no mitosis was detected in GCT. Mean Ki-67 index was <1% in PO and GCT, and 4.8% in SCO. Mean follow-up was 37 months (range of 3-129 months). Two SCOs recurred at follow-up, after 36 and 106 months from surgery, respectively. The remaining patients are alive without disease.

Conclusions: PO and GST appear more benign outcome than SCO. Long-term and strict clinical and neuroimaging follow-up is crucial.

1701 The Use of Optical Coherence Tomography to Assess Peri-Ocular Skin Cancers: An Optical Biopsy

Sabrina Bergeron[1], Bryan Arthurs[2], Debra-Meghan Sanft[3], Miguel Burnier[4]
[1]The MUHC - McGill University Ocular Pathology Laboratory & Translational Research Laboratory, Montreal, QC, [2]McGill University, Montreal, QC, [3]McGill University, Montréal, QC, [4]MUHC - McGill University Ocular Pathology Laboratory, Montreal, QC

Disclosures: Sabrina Bergeron: None; Bryan Arthurs: None; Debra-Meghan Sanft: None; Miguel Burnier: None

Background: Non-melanoma skin cancer (NMSC) is the most common malignancy in adults and its incidence is increasing worldwide. These lesions develop predominantly on sun-exposed areas such as the head and neck; about 20% will affect the peri-ocular region.

Management of NMSC is generally limited to visual inspection followed by excision of the lesion. However, some of these lesions are particularly challenging and the rate of clinical misdiagnosis is estimated at 20%, in addition to an estimated 12% rate of false negative due to small biopsy size.

Our aim is to validate the use of optical coherence tomography (OCT), a non-invasive imaging modality, to assess peri-ocular skin cancers prior to their excision.

Design: Fifty patients with peri-ocular skin lesions suspicious of malignancy were enrolled in our study. OCT images (Optovue, Fremont CA) of the lesion and its contra-lateral side were acquired before the surgical intervention. Each diagnostic was histopathologically confirmed as per normal standard of care and the OCT images were then correlated to their corresponding histopathological sections.

Results: From the OCT images, a total of six features that are comparable to histopathology were identified; hyper-reflective superior band, acanthosis, loss of dermal-epidermal junction, hypo-reflective nest with or without surrounding halo, hyper-reflective nest and cystic spaces.

The presence of hypo-reflective nests with a surrounding halo is strongly linked to the diagnostic of basal cell carcinoma (present in 82% of BCC). In two cases where the clinical diagnosis did not match the histopathological diagnosis, the OCT images were in agreement with the histopathology. In both patients, the presence or absence of hypo-reflective nest on OCT was of diagnostic significance.

Conclusions: Our findings show how OCT imaging can enhance clinical acumen and guide the biopsy site. We prove that hypo-reflective nests on OCT is strongly linked to basal cell carcinoma and can potentially be used on a rule-in or rule-out basis to facilitate patient's referral to oculoplastic services.

OCT is a well-established and non-invasive imaging modality that requires no tissue preparation; it is also accessible in all eye care clinics. Implementing OCT imaging will contribute to reduce the rate of clinical misdiagnosis and the number of repeat biopsies. We recommend that ophthalmic pathologists discuss OCT imaging with their oculoplastic surgeon, together working towards more efficient and better patient care.

1702 ABCB1, ABCC1 AND ABCG2 Transporters Expression in 180 Primary Retinoblastoma

Lourdes Cabrera-Muñoz[1], M Ponce[2], Stanislaw Sadowinski-Pine[3], Orjuela Manuela[4], Alejandro Gomez[5], Ofelia Loyola[5]
[1]Hospital Infantil de Mexico Federico Gomez, Mexico City, Mexico, [2]CMN SXXI, Hospital de Pediatría IMSS, Mexico, Cuauhtémoc, Mexico, [3]Hospital Infantil de Mexico Federico Gomez, Alcaldia Cuauhtemoc, Ciudad de México, Mexico, [4]Columbia University, New York, NY, [5]CMN SXXI, Hospital de Pediatría IMSS, Alcaldia Cuauhtemoc, Ciudad de México, Mexico

Disclosures: Lourdes Cabrera-Muñoz: None; M Ponce: None; Stanislaw Sadowinski-Pine: None; Ofelia Loyola: None

Background: Retinoblastoma (RB) is an intraocular malignant tumor that originates in the retina during early childhood. There are two forms of the disease unilateral o bilateral. Extraocular disease is associated to poor survival. ABC transporters are integral membrane proteins, form a family of more 40 members. ABCB1 (P-gp), ABCC1 (MRP), y ABCG2 (BCRP) had been associated to chemotherapy resistance in diverse solid tumors of adults. There are only a few works reporting the expression of these transporters in RB. The aim of this work was to determine ABCB1, ABCC1 y ABCG2 expression in primary RB and to explore if a correlation do exist with laterality or patients gender.

Design: In this work, 180 patients diagnosed with RB and treated with enucleation were included; from two large Pediatric hospitals in Mexico City. From those 110 were unilateral and 70 bilateral, 93 male and 88 female. Six tissue microarrays were constructed to explore by IHC the expression of this transporters using a semi quantitative scale.

Results: From a total of 180 patient, 110 were unilateral (65 male, 45 female) and 70 were bilateral (28 male, 42 female). Immunohistochemical results and clinical data is presented in the table. Statistical test OD >2.4 (95% CI 1.27-4.77) show that only ABCB1 is associated to bilateral cases, No association was found with gender; neither to chemotherapy prior to enucleation. Multivariated analysis show that 8 cases expressed the three transporters and 33 cases expressed two transporters and no association was found to oncological stage.

Transporter	+	++	+++	Case/total	%	Male%	Female%	Uni%	Bi%
ABCB1	14	19	22	55/181	30%	26	30.6	20.9	**39.4**
ABCC1	8	16	11	35/181	19%	21.5	17	21.8	15.4
ABCG2	11	22	27	60/181	33%	35.4	29.5	31.8	33.8

Conclusions: Considering that efforts to save the remaining eye in bilateral cases are part of modern treatment, detection of ABCB1 transporter protein in the first enucleated eye, can justify the use of ABCB1 blockers like verapamil in the treatment of the second eye.

1703 Primary Intracranial Pediatric Sarcoma of the CNS with DICER1 Mutation in Peru. Multicenter Retrospective Analysis

Sandro Casavilca Zambrano[1], Rosdali Diaz[1], Christian Koelsche[2], Fiorela Mego Ramirez[3], Juan García[1]
[1]Instituto Nacional de Enfermedades Neoplásicas, Lima, Peru, [2]Ruprecht-Karls-University Heidelberg, Heidelberg, Germany, [3]Lima, Peru

Disclosures: Sandro Casavilca Zambrano: None; Christian Koelsche: None

Background: The 2016 World Health Organization (WHO) classification of tumors of central nervous system (CNS), classifies sarcomas into the group of non-meningothelial mesenchymal tumors, which presumably arise from mesenchymal progenitor cells within the meningeal cover of the brain and along the perivascular spaces of Virchow-Robin . It has a wide range of age of presentation in childhood and adults between 1 week and 75 years. Most reports of primary brain sarcomas arise in the pediatric population. The causes are not well established, but hereditary syndromes and ionic radiation are included. In recent years in Peru, we have had an unusually high incidence of spindle cell sarcomas and pleomorphic sarcomas, not otherwise specified, and in previous reports, we found in most of them somatic tumor mutations in the Dicer1 gene. Other affected genes were the NF1 gene or the P53 gene mutation in approximately 20% of the cases studied.

Design: Patients with histological diagnosis of CNS-Sarcoma from The National Cancer Institute in Peru (INEN, "Instituto Nacional de Enfermedades Neoplásicas") and other Private Centers (Clinica Delgado and Clinica Angloamericana); were centrally reviewed by an expert Neuropathologist to confirm and included in a database. Formalin-fixed, paraffin-embedded tumor tissue was collected for all cases where this was available (n=29). Patients with FFPE-tumor tissue available that were in contact with the participating sites were asked to provide a blood sample (n=20). Next-generation panel sequencing of DNA obtained from FFPE tumor tissue and peripheral blood was performed.

Results: DNA methylation profiling 28 tumors was done. Using the Heidelberg brain tumor classifier v11b4, none of the DNA methylation profiles of the tumors matched with any of the previously described reference classes. Using the Heidelberg Sarcoma classifier, all cases matched to the recently described class "primary intracranial sarcoma with rhabdomyosarkoma-like features, DICER1 mutant".

On panel sequencing was available for 26/28 cases. For one case, Exome sequenceing results were available from another institution and thus panel sequencing was not repeated. In all but one case a DICER1-mutation was identified, 22/27 cases had an additional TP53 mutation. Strikingly, none of the DICER1 or TP53 mutations identified in tumor tissue were found to be germline events in the 19 cases where blood as germline control was available despite 13/26 patients carrying more than one somatic mutation in DICE

Age [years]	Median	8
	Range	1.0 – 21.0
	[1-7]	15
	[8-14]	12
	[15-21]	2
Sex	M	19
	F	10
Localization	Pontocerebelous Angle	1
	Bifrontal	1
	Frontal Rigth	3
	Frontal Left	7
	Fronto Parietal Left	2
	Fronto Temporal Left	1
	Frontoparietotemporal Right	1
	Occipital Left	1
	Parietal Rigth	2
	Parietal Left	2
	Parieto Occipital Left	1
	Parieto Temporal Left	1
	Temporal Rght	2
Tratamient	QT+RT	13
	QT	0
	RT	2
	NONE	8
	ND	4
OUTCOME	Alive	9
	Death	16
	ND	4
	Alive - M	6
	Death- M	12
	Alive - F	3
	Death - F	4
NF1mut	somatic	6
	germline + somatic	1
	WT	19
	NA	1
DICER1mut	single (somatic)	13
	double (somatic)	1
	WT	12
	NA	1
Tp53mut	somatic	5
	WT	21
	NA	1

Figure 1 - 1703

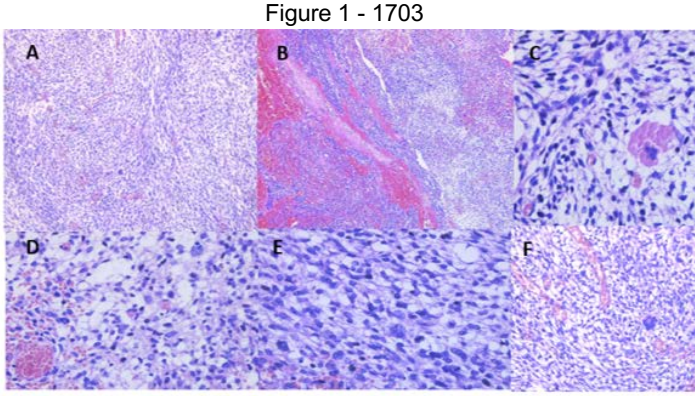

IMAGES H&E OF INTRACRANIAL SPINDLE CELL SARCOMA A.- STORIFORM TUMORAL PATTERN OF INTRACRANEAL SPINDLE CELL SARCOMA B.- HEMORHAGIC AREAS IN SPINDLE CELL SARCOMA (OBJETIVE 5X) C.- EOSINPHILIC GRANULAR INTRACITOPLASMATIC MATERIAL (C INTRACITOPLASMIC HYALINE GLOBULES (OBJETIVE 40X) E.- MITOTIC ACTIVITY AND CYTOPLASMATIC VACUOLIZATION (OBJETIVE 40X) SOME PLEOMORPHIC MULTINICLEATED CELLS (OBJETIVE 20X)

Figure 2 - 1703

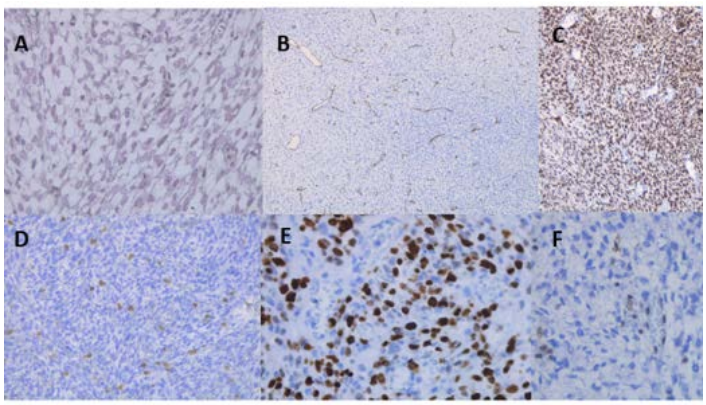

INMUNOHISTOCHEMESTRY OF INTRACRANIAL SPINDLE CELL SARCOMA A.- FINE PERICELLULAR DEPOSITS OF RETICULINE (OBJETIVE 40X) B.- CD 34 HEMANGIOPERICITOID PATTERN (OBJETIVE 10X) C.-P53 WITH DIFUSE POSITIVE NUCLEAR EXPRESSION (OBJETIVE 40X) D.- CYTOPLASMIC EXPRESSION IN SPAR 20X) E.-MIB-1 HIGH PROLIFERATIVE INDEX OF 50% OF TUMORAL CELLS WITH NUCLEAR EXPRESSION OF MIB-1 (OBJETIVE 40X) F.- ATRX LOST OF NUCLE TUMORAL CELLS (OBJETIVE 20X)

Conclusions: In our opinion this tumor is not a rhabdomyosarcoma, however, we can find myogenic differentiation and rhabdomyoblastic markers in some cases. Apparently there is a morphological spectrum that goes from spindle cell / pleomorphic and undifferentiated not classified sarcoma, some of them with heterologous differentiation that includes chondroid malignant component. In the lasts, years his incidence is unusually increased and requires multidisciplinary studies that include not only molecular profiles but also epidemiological and environmental studies that try to explain what factors could be related with this phenomenon.

1704 Characterization of Trop-2 and 5-HMC Expression in Benign, Atypical and Anaplastic Meningiomas

Corey Chang[1], Serguei Bannykh[1], Xuemo Fan[1]
[1]Cedars-Sinai Medical Center, Los Angeles, CA

Disclosures: Corey Chang: None; Serguei Bannykh: None; Xuemo Fan: None

Background: Trophoblast transmembrane glycoprotein-2 (Trop-2) is highly expressed in many cancer types and plays a role in proliferation, survival, self-renewal and invasion. 5-hydroxymethylcytosine (5-HMC) is believed to play a role in epigenetic regulation. The pattern of Trop-2 and 5-HMC expression in different subsets of meningiomas remains to be determined.

Design: Formalin-fixed, paraffin-embedded tissue sections from benign (n=16), atypical (n=16) and anaplastic meningiomas (n=16) were retrieved from departmental archives at Cedars-Sinai Medical Center. Representative H&E slides were re-reviewed to confirm diagnosis. Immunostains for Trop-2 and 5-HMC were performed. Positive staining for Trop-2 was defined as dark membranous staining pattern and was further stratified based on intensity of stain (0 = negative; 1+ = faint, 2+ = light; 3+ = dark). Positive staining for 5-HMC was defined as a dark red nuclear staining pattern and was further semiquantified based on nuclear staining pattern (0 = negative; 1+ = faint ; 2+ = light; 3+ = dark). For 5-HMC immunostain, three patterns of extent of staining were noted (retained = greater than 50%; "mosaic pattern" = 5-50% positive nuclei; loss = <5% positive nuclei). One-way nonparametric ANOVA analysis (Kruskal-Wallis test) was performed across the three groups and a p-value <0.05 was considered significant.

Results: Ten out of sixteen (10/16) anaplastic meningiomas show focally increased Trop-2 staining. Staining intensity varied within this group with two showing strong 3+ staining, two with light 2+ staining and the remaining 6 with faint 1+ staining. Six of the sixteen (6/16) benign meningiomas show focal 1+ staining. Three of the sixteen (3/16) atypical meningiomas show focal 1+ staining. All sixteen (16/16) benign meningiomas show a retained nuclear 5-HMC staining. Eleven of the sixteen (11/16) atypical meningiomas show a retained pattern; the remaining five show a mosaic pattern. Six of the sixteen (6/16) anaplastic meningiomas show a retained pattern, five show mosaic pattern and five show loss.

Figure 1 - 1704

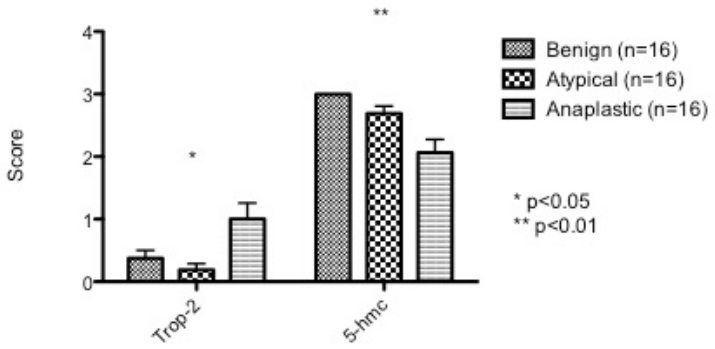

Conclusions: In contrast to benign and atypical subtypes, anaplastic meningiomas demonstrate decreased 5-HMC and increased Trop-2 staining. Increased Trop-2 expression in anaplastic meningioma raises the possibility that those patients may potentially be treated with Sacituzumab govitecan (IMMU-132), an antibody–drug conjugate (ADC) made from anti-Trop-2 monoclonal antibody. Additional studies are needed to confirm our initial findings.

1705 CSF Cytokine Profiles Help Discriminate CNS Tumors, Lymphomas, Autoimmune Diseases, and Infections

Timothy Chao[1], Danielle Fortuna[2], Rhonda Kean[1], Douglas Hooper[1], Michelle Nagurney[1], Mark Curtis[1]
[1]Thomas Jefferson University Hospital, Philadelphia, PA, [2]Hospital of the University of Pennsylvania, Philadelphia, PA

Disclosures: Timothy Chao: None; Danielle Fortuna: None; Rhonda Kean: None; Douglas Hooper: None; Michelle Nagurney: None; Mark Curtis: None

Background: The clinical presentation and imaging features of certain types of central nervous system (CNS) disorders often overlap, significantly delaying appropriate therapy. Although they are useful in identifying CNS bacterial infections, routine cerebral spinal fluid (CSF) white blood cell (WBC) count, protein, and glucose levels are often inadequate to discriminate CNS tumors, lymphomas, autoimmune diseases, and infections. This inability to rapidly discriminate among CNS disease types not only leads to excessive laboratory testing but may also result in the initiation of inappropriate therapy. We have previously shown that CSF cytokines may help to rapidly distinguish infectious from non-infectious CNS disorders. Here we examined the potential of using CSF cytokines to discriminate patients with tumors, lymphomas, autoimmune diseases, and infections in the CNS.

Design: We quantified 41 CSF cytokine levels in adult patients with CNS tumors (n=10), autoimmune diseases (n=8), lymphomas (n=5), infections (n=3), and systemic disease without CNS involvement (n=15). Agglomerative hierarchical clustering (AHC) and linear discriminant analysis (LDA) were used to demonstrate whether CSF cytokine levels could distinguish samples by CNS disease type. The Kruskal-Wallis and post-hoc Mann-Whitney tests were used to determine significant differences. Unbiased random forest machine learning then selected cytokines with the highest ability to discriminate the CNS disease classes. Finally, we compared the accuracy of a decision tree built with the selected cytokines to a tree constructed using routine CSF values.

Results: An AHC generated heat map demonstrated distinct cytokine profiles for the different CNS disease types. LDA revealed robust cytokine-dependent patient sample clustering by CNS disease type. Of the 41 cytokines analyzed, 24 showed significant differences among the CNS disease classes. An unbiased algorithm then identified five cytokines (IL-6, IL-10, IL-8, MDC, and GRO) as having the highest discriminatory power among the different CNS disease types. A decision tree with these cytokines significantly outperformed a tree using routine CSF values (accuracy 82.9% vs 65.8%).

Conclusions: We demonstrate that CSF cytokine profiles of various CNS disease are distinct. Therefore, CSF cytokine-based algorithms hold clinical potential to rapidly identify the CNS disease class afflicting patients and to facilitate timely initiation of appropriate therapy.

1706 Evaluation of Prognostic Values of Perivascular Lymphocyte Cuffing and Microglia-Macrophage Infiltrate in a Series of Glioblastomas

Alessia Cimadamore[1], Antonio Zizzi[2], Laura Pepi[2], Rodolfo Montironi[3], Marina Scarpelli[4]
[1]Università Politecnica delle Marche, Ancona, Marche, Italy, [2]Section of Pathological Anatomy, Polytechnic University of the Marche Region, School of Medicine, United Hospitals, Ancona, Italy, [3]University Politecnica delle Marche/Medicine, Ancona, Italy, [4]Torrette, Ancona, Italy

Disclosures: Alessia Cimadamore: None; Antonio Zizzi: None; Laura Pepi: None; Rodolfo Montironi: None; Marina Scarpelli: None

Background: Glioblastomas (GBM) are aggressive tumors associated with very poor prognosis. Presence of lymphocytic inflammatory infiltrate and presence of microglia and tumor associated-macrophages have been postulated to be associated with prognosis. The present study aims to evaluate the prognostic values of the perivascular lymphocyte cuffing (PLC) and of the microglia/macrophages inflammatory infiltrate in a series of GBM.

Design: This single-institution retrospective study included 102 patients who underwent tumor resection from 2012 through 2017. All the FFPE blocks and H&E sections available for each patients were retrieved from our archive and revaluated for presence of perivascular lymphocyte cuffing (PLC)(Figure 1). In the young patients 'subset (< 55 years old) the evaluation of microglia and macrophages infiltrate was evaluated by immunohistochemical stains for CD68 (resting microglia and macrophages M1) and CD163 cells (activated microglia and macrophages M2 pro-tumorigenic phenotype). The infiltrate was defined intense-moderate/mild-absent using a qualitative approach. Blinded evaluation was performed independently by two pathologists. IDH gene mutations were evaluated first by IHC and then by gene sequencing in all patients.

Results: Patients age ranged from 22 to 68 years (mean: 64 years). 21 patients were younger than 55 years at time of diagnosis. The overall survival (OS) was of 12 months (median follow-up 18 months). 51% (52/102) of patients showed presence of PLC. Ninety-eight were IDH wild-type GBM. Four glioblastomas harbored mutation for IDH gene: two harbored the classical mutation IDH1 R132H assessed by IHC and confirmed with gene sequencing, the other two harbored IDH1 R132G and IDH2 R172K, both assessed by gene sequence analysis. None of these IDH-mutated tumors presented PLC. Overall, the presence of PLC was associated with an improved OS (p=0,0263)(Figure 2). No association was found between IDH 1/IDH 2 mutation and presence of PLC. The evaluation of the microglia/macrophage infiltrate showed a group of tumors with intense/moderate CD68 and CD163 positive cells infiltrate and a group with mild/absent infiltrate. No association was found between the microglia/macrophage infiltrate and OS

Figure 1 - 1706

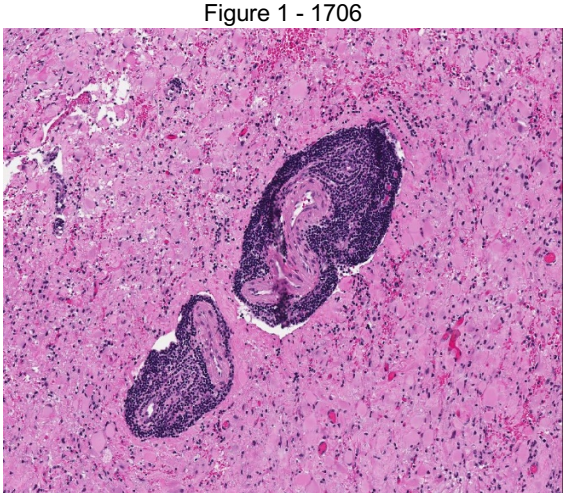

Figure 2 - 1706

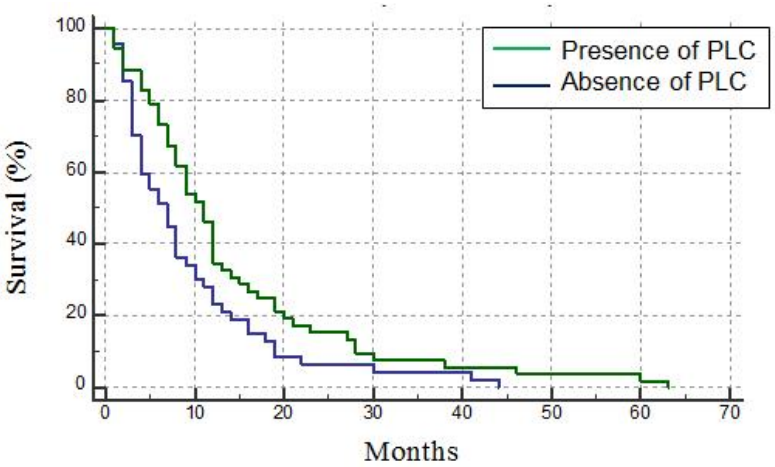

Conclusions: Although the sample size for the study is limited, the presence of PLC demonstrated to be a positive prognostic parameter in GBM patients. The elicitation of the inflammatory response against tumor cells may be a potential treatment strategy for these aggressive tumors.

1707 Clinicopathologic Features of Low-Grade Astrocytoma with QKI-RAF1 Fusion: Histologic and Clinical Similarities in Three Pediatric Cases

Jennifer Cotter[1], Ashley Margol[1], Benita Tamrazi[1], Jianling Ji[1]
[1]*Children's Hospital Los Angeles, Los Angeles, CA*

Disclosures: Jennifer Cotter: None; Ashley Margol: None; Benita Tamrazi: None; Jianling Ji: None

Background: Fusions of QKI with MYB have been described in astrocytomas with alteration of MYB presumed to be the oncogenic driver. Likewise, "diffuse glioma, MYB-altered," is a recommended distinct diagnosis in a recent update from cIMPACT-NOW. The role of QKI is not as well understood, but QKI has a known oncogenic effect via the PI3K pathway. At our institution we have identified three pediatric brain stem astrocytomas harboring gene fusion of QKI and RAF1 (a.k.a. CRAF). MAP kinase pathway alterations including RAF1 rearrangement are described in pilocytic astrocytoma, but QKI-RAF1 fusion is very rare, with only four previously described cases. RAF1 gene fusions may be of therapeutic significance, as there is in vitro evidence of response to co-targeting with MEK inhibitors and mTOR

inhibitors. Overall the incidence, clinical presentation, and imaging features of astrocytomas with QKI-RAF1 fusions are not well-established.

Design: By next-generation sequencing (OncoKids(R)) on clinical tumor specimens, we identified three cases of low-grade astrocytomas harboring QKI-RAF1 fusion with 3-8 breakpoints and retained RAF1 kinase domain. Available clinical, histologic, and molecular genetic features were compiled. We reviewed existing literature and identified four other described glial tumors with QKI-RAF1 fusion.

Results: All three QKI-RAF1 cases at our institution occurred in the brain stem of young children (ages 3, 3, and 6). The histologic features in all cases are consistent with low-grade astrocytoma with an infiltrative growth pattern; two cases had pilocytic features including Rosenthal fibers and eosinophilic granular bodies. Radiologically, tumors had some characteristics of pilocytic astrocytoma with some atypical and more aggressive features.

Previously reported cases with QKI-RAF1 fusion include a pilocytic astrocytoma in the diencephalon of a 5-year-old girl, a spinal cord pleomorphic xanthoastrocytoma in a 49-year-old man, an oligodendroglioma and a pilocytic astrocytoma with unknown clinical features.

Conclusions: Low-grade astrocytoma with QKI-RAF1 fusion may be an emerging entity in the category of pediatric low-grade astrocytoma. At our institution the three identified cases have striking clinical similarities in age and location, and imaging features are also similar among the three cases. Future identification of such cases will deepen our understanding of this subgroup of low grade astrocytomas, including their clinical behavior and potential therapeutic options.

1708 Global Activation of Oncogenic Pathways Underlies Therapy Resistance in Diffuse Intrinsic Pontine Glioma

Maria-Magdalena Georgescu[1], Yan Li[2], Mohhammad Islam[3], James Traylor[4], Dennis Burns[5]
[1]NeuroMarkers PLLC, Houston, TX, [2]LSU Health Shreveport, Shreveport, LA, [3]LSU Health Sciences Center, Shreveport, LA, [4]LSUHSC-Shreveport, Shreveport, LA, [5]University of Texas Southwestern Medical Center, Dallas, TX

Disclosures: Maria-Magdalena Georgescu: None; Yan Li: None; Mohhammad Islam: None; James Traylor: None; Dennis Burns: None

Background: Diffuse intrinsic pontine gliomas (DIPGs) are very aggressive pediatric brain tumors that usually harbor the histone H3 K27M mutation and are classified within the new WHO grade IV category of diffuse midline gliomas K27M-mutant. Despite multiple modalities of treatment, the patient prognosis is dismal due to tumor spread and establishment of therapy-resistant secondary foci.

Design: We performed the first integrated histologic, genomic and proteomic analysis of three highly invasive DIPGs in a total of 15 infratentorial and 6 supratentorial foci, representing the largest analysis of matched supratentorial foci to date.

Results: Histone H3.3 K27M was the driver mutation in all foci, in combination with other somatic oncogenic mutations or germline variants in *ATM* or *MYCN* genes. Somatic oncogenic mutations mapping to previously reported genes – *TP53*, *ATM, ATR, PPM1D*, *ASXL1*, *KDM6A, PIK3CA*, *PIK3R1*, *KRAS, NF1*, *PDGFRA,* were variably detected, either in isolated foci or across all tumor. Pathogenic copy number variation or loss-of-function mutations were detected in a new category of genes involved in differentiation, including *TCF12*. The proteomic analysis showed global upregulation of histone H3 expression with downregulation of the PRC2 complex modifier ASXL1, lack of histone H3.3 K27 methylation, and N-Myc upregulation. Global activation of oncogenic pathways resulted either from protein upregulation in the case of p65/p50 NF-kB, EGFR/CD44/MAPK, and STAT3 pathways, or from combined PDGFR/PI3K mutations and PHLPP1 tumor suppressor downregulation for the PI3K/AKT pathway. Focal activation, mainly of cell invasion pathways, such as Src and FAK, was also detected.

Conclusions: The integrated histologic, genomic and proteomic analysis allowed spatial and temporal modeling of tumor progression and delineated common signaling pathways and potential therapeutic targets activated in all foci. It also revealed an unsuspected overwhelming activation of a multitude of oncogenic pathways, potentially explaining the resistance to therapy of DIPG.

1709 Beyond IDH1 R132H Mutation: Characteristics of Non-Canonical IDH Mutant Gliomas

Mario Giner Pichel[1], Rosa Somoza[2], Griselda Venturas[3], Jessica Camacho[4], Ana Aula Olivar[5], Luisa Sofía Silva Alcoser[1], Cristina Auger[1], María Vieito[6], Francisco Martínez-Ricarte[1], Xavier Maldonado[1], Santiago Ramon Y Cajal[1], Javier Hernandez-Losa[7], Elena Martinez-Saez[1]

[1]Vall d'Hebron University Hospital, Barcelona, Spain, [2]Vall d'Hebron Institute Research, Barcelona, Spain, [3]1. Vall d'Hebron University Hospital, Barcelona, Spain, [4]Barcelona, Spain, [5]Vall d'Hebron University Hospital (HUVH), Barcelona, Spain, [6]1. Vall d'Hebron Research Institute (VHIR), Barcelona, Spain, [7]1. Hospital Universitari Vall d'Hebron. 2. VHIR. 3. CIBERONC, Barcelona, Spain

Disclosures: Mario Giner Pichel: None; Rosa Somoza: None; Griselda Venturas: None; Jessica Camacho: None; Ana Aula Olivar: None; Luisa Sofía Silva Alcoser: None; Cristina Auger: None; María Vieito: None; Francisco Martínez-Ricarte: None; Xavier Maldonado: None; Santiago Ramon Y Cajal: None; Javier Hernandez-Losa: None; Elena Martinez-Saez: None

Background: Isocitrate-dehydrogenase (IDH) mutations are the most important molecular alteration in infiltrating gliomas, leading to the 2016 WHO classification into “IDH-mutant” and “IDH-wt” entities. The p.R132H mutation is the most frequent change, but around 10% of IDH mutations are “non-canonical” (ncIDHmut, such as p.R132C, p.R132S, p.R132L and p.R132G in the *IDH1* gene, and p.R172K, p.R172G and p.R172M in the *IDH2* gene). The aim of this study is to investigate the epidemiological and morphological characteristics of these non-canonical mutations in our reference population.

Design: Infiltrating gliomas diagnosed at the Vall d’Hebron Pathology Department were reviewed according to the 2016 WHO guidelines. IDH1 R132H, ATRX and p53 immunohistochemistry was performed in all cases, 1p/19q FISH study and *IDH1/2 gene* sequencing when required. Clinical charts were reviewed.

Results: 296 gliomas were thoroughly studied (55 grade II, 29 grade III and 212 grade IV). *IDH* mutations were found in 26,3% of cases (78/296), with 18 cases of non-canonical *IDH* mutations (6%). These mutations were more prevalent in *IDH1* (11/18: 5 p.R132C, 3 p.R132G, 1 p.R132S and 1 p.R132L) than in *IDH2* (7/18: 5 p.R172K, 1 p.R172M, 1 p.R172W). As expected, patients with IDHmut were significantly younger than those with IDHwt (41,2 yo vs 56,08 yo, p<0,001), and patients with ncIDHmut represented the youngest group (36,7 yo), specially IDH2mut (35,4 yo). Histologically, all ncIDH1 mutations corresponded to astrocytic tumours, and surprisingly all ncIDHmut oligodendrogliomas harboured an IDH2 R172K mutation. The main morphological features in ncIDHmut cases were: oligo-like cells (83,3%), thin-walled cysts (47% of ncIDHmut, and 71,4% of IDH2mut) and alveolar-like spaces (31,2%).

Conclusions: Non-canonical IDH mutations represent a non-negligible event with diagnostic and prognostic implications, and seem to have distinct clinical and histological characteristics (affecting younger patients than the classical p.R132H mutation, with an association between oligodendroglioma and p.R172K mutation in our reference population). Their detection should be part of the diagnostic workup of infiltrating gliomas, particularly with the emergence of IDH-based clinical trials in gliomas.

1710 Evidence of NTRK2 Fusions by Copy Number Aberrations

Abigail Goodman[1], Bryan Morales[2], Matthew Schniederjan[3], Jose Velazquez Vega[4], Pia Mendoza[2], Stewart Neill[5]

[1]Emory University Hospital, Atlanta, GA, [2]Emory University School of Medicine, Atlanta, GA, [3]Emory University & Children's Healthcare of Atlanta, Atlanta, GA, [4]Children's Healthcare of Atlanta, Atlanta, GA, [5]Emory University Medicine, Decatur, GA

Disclosures: Abigail Goodman: None; Bryan Morales: None; Matthew Schniederjan: None; Jose Velazquez Vega: None; Pia Mendoza: None; Stewart Neill: None

Background: Several types of cancer harbor gene fusions involving the neurotrophic tyrosine kinases (NTRK), and recently novel agents targeting tropomyosin receptor kinases (TRK) have become available. Current clinical data is promising that these agents can be highly effective in patients with tumors harboring NTRK gene fusions. However, only 1% of all solid tumors are estimated to harbor an NTRK gene fusion, thus screening all tumors for a NTRK fusion could be relatively cost prohibitive. An immunohistochemical marker to detect TRK-fused lesions is available but is not useful in all tumor types. Here we report 3 cases of primary brain tumors in which an NTRK2 fusion was suggested by routinely performed chromosomal microarray and confirmed by molecular assays specifically designed to detect NTRK fusions.

Design: We routinely perform chromosomal microarray using an FFPE based molecular inversion probe assay (Oncoscan Array, ThermoFisher) on brain tumor cases for clinical purposes to detect diagnostically relevant copy number aberrations. Oncoscan Array is a whole-genome copy number microarray-based assay that enables the detection of relevant copy number aberrations, such as copy number gain and loss and loss of heterozygosity. Copy number aberrations terminating within know cancer genes may suggest associated rearrangements.

Results: In 3 primary brain tumors aberrations in copy number were noted in the NTRK2 gene. The first case demonstrated an amplification of NTRK2 with a nearby copy number gain breaking within KIF27, the second case demonstrated a gain and loss involving NTRK2, and third case showed a subtle copy number gain within NTRK2. Confirmatory testing for an NTRK2 fusion was performed and demonstrated an NTRK2 fusion in all 3 cases, with different fusion partners in each case.

Conclusions: NTRK2 fusions have been reported to occur in a variety of brain tumors. However, the frequency of these fusions is low, thus specific NTRK fusion testing is not routinely performed in many labs. Here we provide evidence that assessment of copy number variation within the NTRK genes by orthogonal methods may help identify patients in whom directed NTRK fusion testing may be beneficial. One of the patients identified in this cohort was treated with entrectinib, a CNS-active TRK inhibitor, and demonstrated a period of marked response. Overall, more comprehensive study will be necessary to determine the exact efficacy of this testing approach.

1711 Molecular Analysis of Epithelioid Glioblastomas Lacking BRAF V600E Mutation

Sneha Gupta[1], David Meredith[2]
[1]*Brigham and Women's Hospital, Morgantown, WV,* [2]*Boston, MA*

Disclosures: Sneha Gupta: None; David Meredith: None

Background: Epithelioid glioblastoma (eGBM) is a rare morphologic variant of glioblastoma recently described in the 2016 WHO Classification of Tumors of the Central Nervous System. Previous studies have established that *BRAF V600E* mutations are present in around 50% of eGBMs and correlate with improved survival relative to other *IDH1/2* wild-type glioblastomas. The behavior and genomic landscape of eGBMs lacking *BRAF* mutations; however, remains poorly understood. In this study, we identified eGBMs lacking *BRAF V600E* mutations and comprehensively reviewed molecular data to further describe these tumors.

Design: 20 non-*BRAF* mutated eGBMs were identified in routine surgical and consultation archives with available chromosomal microarray and/or targeted exome sequencing data.

Results: Microscopically, all tumors showed a predominantly epithelioid or rhabdoid morphology with abundant mitotic activity, vascular proliferation and/or necrosis. Eosinophilic granular bodies, Rosenthal fibers, bizarre atypia, and xanthomatous change were absent. *MGMT* promoter methylation was identified in 6/17 cases. Approximately two-thirds of cases showed a classic glioblastoma signature, including polysomy of chromosome 7, loss of 9p (*CDKN2A/B*), and loss of chromosome 10. Amplification of *EGFR* was detected in 35% of cases, while 30% of cases also showed monosomy of chromosomes 13 and 22. Somatic mutation testing revealed that 40% of tumors harbored *TERT* promoter mutations and *PTEN* loss of function mutations. Interestingly, many tumors showed alternative means of activating the MAPK pathway via loss-of-function mutations in *TSC1/2* (20%), amplification of *BRAF/KRAS/HRAS* (15%), or activating mutations in *RAF1* (5%) or *RET* (5%). Additionally, 6 tumors showed focal gains of 9p24 (including *CD274* and *PDCD1LG2*), a finding not previously reported in gliomas. Immunohistochemistry for PD-L1 confirmed subclonal overexpression in 4 of these cases in which tissue was available.

Conclusions: These results indicate that non-*BRAF* mutated eGBMs possess frequent activation of the MAPK pathway and overexpression of PD-L1/2 within an overall conventional glioblastoma genomic signature.

1712 Prognostic Value of BAP1 and PRAME Immunohistochemistry in Uveal Melanomas

Lucy Han[1], Michele Bloomer[1], Melike Pekmezci[1]
[1]*University of California San Francisco, San Francisco, CA*

Disclosures: Lucy Han: None; Michele Bloomer: None; Melike Pekmezci: None

Background: Uveal melanoma (UM) is the most common primary intraocular tumor in adults and despite excellent local control, more than 50% of patients develop and die of metastatic disease. Superior to traditional TNM staging, the molecular landscape of UM risk-stratify patients into low-, intermediate- and high-risk for metastasis. It is well understood that loss of BAP1 expression is associated with poor prognosis and high metastatic potential. More recently, the antigen PRAME has been identified as an additional prognostic marker and overexpression of PRAME mRNA, as assessed by RT-PCR is associated with poor prognosis. The purpose of this study is to evaluate the BAP1 and PRAME expression in UM by immunohistochemistry (IHC) and assess their prognostic roles.

Design: We have retrospectively reviewed 107 uveal melanoma cases with sufficient tissue. Clinical data about treatment, presence and time to recurrence, and presence and time to metastasis were collected from electronic medical records. IHC for BAP1 and PRAME were performed on whole slide sections of 12 cases with limited tissue, and on tissue microarrays (2 mm duplicate cores) on 95 cases. BAP1 was scored as lost if there is no nuclear staining in the tumor cells in the presence of positive internal control. PRAME was scored as positive if there was any degree of nuclear staining.

Results: Forty-three (40%) cases were BAP1-retained/PRAME-negative (group 1), 14 (13%) cases were BAP1-retained/PRAME-positive (group 2), 33 (31%) cases were BAP1-lost/PRAME-negative (group 3) and 17 (16%) cases were BAP1-lost/PRAME-positive (group 4). Follow-up was available in a subset of cases with a median follow-up time of 2 years. The rate of metastasis was 1/24 (4%) among group 1, 1/5 (20%) among group 2, 5/16 (31%) among group 3 and 6/10 (60%) among group 4 patients. While the association between the metastatic rate and group showed a trend, there was no statistical difference likely due to small sample size and limited follow-up period. No difference in stage was identified between groups.

Conclusions: Group 4 (BAP1-lost/PRAME-positive) cases comprise approximately 16% of UM in our cohort and had a 60% metastasis rate, far exceeding that of all other cases in this cohort. Among tumors with retained BAP1 expression, group 2 (PRAME-positive) cases have a higher metastasis rate than group 1 (PRAME-negative) cases, suggesting an intermediate prognosis for group 2 tumors. This is consistent with the results based on mRNA expression studies. Combination of BAP1 and PRAME stains may be helpful to provide prognostic information for uveal melanomas.

1713 Medulloblastomas with Hybrid Molecular Features

Jeffrey Helgager[1], Peter Pytel[2], Eudocia Lee[3], Matija Snuderl[4], J. Bryan Iorgulescu[5], Keith Ligon[6]
[1]Brigham and Women's Hospital, Harvard Medical School, Brookline, MA, [2]University of Chicago Medicine, Chicago, IL, [3]Dana-Farber Cancer Institute, Harvard Medical School, Boston, MA, [4]New York University, New York, NY, [5]Boston, MA, [6]Brigham and Women's Hospital, Boston, MA

Disclosures: Jeffrey Helgager: None; Peter Pytel: None; Matija Snuderl: None; J. Bryan Iorgulescu: None

Background: Molecular characterization of CNS tumors is becoming increasingly important for both diagnostic clarity and prognostication in Neuropathology. Medulloblastomas in particular can be divided into four core consensus molecular subgroups—WNT-activated, SHH-activated, Group 3, and Group 4—based on molecular alterations which predict prognostic outcomes better than histology alone. These four distinct molecular subtypes have been thought to be mutually exclusive and homogeneous within individual tumors. Recently, however, five cases of medulloblastoma have been reported which harbor combined molecular alterations characteristic of both WNT and SHH-activated neoplasms, suggesting that there can be overlap between molecular subgroups. Identification of additional such cases is needed to further elucidate the molecular profiles of such hybrid tumors as well as strengthen prognostic and treatment recommendations.

Design: Chromosomal microarray, targeted exome next generation sequencing, and DNA methylation profiling were employed to characterize cases of medulloblastoma possessing alterations of more than one molecular subtype.

Results: We report two cases of medulloblastoma, found at separate institutions, possessing molecular alterations characteristic of both WNT and SHH-activated subtypes. The first was in a 37-year-old female with a CTNNB1 activating mutation and two concomitant PTCH1 nonsense mutations. Strikingly, this case further displayed isochromosome 17q, conventionally thought to be characteristic of Group 3 and Group 4 (G3/G4) medulloblastomas. The second case was in a 29-year-old male, also with a CTNNB1 activating mutation and three PTCH1 nonsense mutations; this case has not recurred 20-months after surgery. DNA methylation profiling demonstrated a profile most consistent with WNT-activated medulloblastoma in both cases, a finding consistent with previously reported WNT/SHH-dual activated neoplasms. This suggests that such tumors are fundamentally WNT-activated with secondarily acquired alterations of other molecular subtypes.

Conclusions: These findings contribute to an increasingly complex molecular classification of medulloblastomas, challenging the notion of mutually exclusive subtypes, and demonstrating additional novel overlap of genotype classes beyond just dual WNT and SHH-activating characteristics. The work further highlights the importance of integrating advanced molecular techniques in the diagnostic classification of CNS tumors.

1714 Genetic Profiling of Circulating Free DNA in Glioma by Targeted Next Generation Sequencing

Nuzhat Husain[1], Sridhar Mishra[2], Adil Husain[2], Mohammad Kaif[3], Rupali Awale[2], Saumya Shukla[2]
[1]Dr Ram Manohar Lohia Institute of Medical Sciences, Lucknow, India, [2]Dr Ram Manohar Lohia Institute of Medical Sciences, Lucknow, Uttar Pradesh, India, [3]Dr Ram Manohar Lohia Institute of Medical Sciences, Lucknow, UP, India

Disclosures: Nuzhat Husain: None; Sridhar Mishra: None; Adil Husain: None; Saumya Shukla: None

Background: Circulating biomarkers for gliomas are still being defined and are not yet in use in clinical practice. Monitoring change in cfDNA level and cfDNA mutation analysis can potentially allow diagnosis and genetic profiling of adult diffuse gliomas (ADG). Titers of cfDNA in ADG were measured to assess their diagnostic potential and next generation sequencing (NGS) in cfDNA was done using in-house designed panels for molecular characterization of ADG.

Design: Study group comprised of 23 biopsy proven cases of adult gliomas including 5 grade II, 3 grade III, 11 grade IV gliomas and 15 healthy individuals. Serum CfDNA was extracted using ChargeSwitch gDNA 1ml Serum Kit (Invitrogen, USA) and quantified using β globin gene amplification. Cut off values for cfDNA diagnostics were calculated from ROC curves. NGS targeted *IDH* gene at COSM28747, COSM28748, COSM28749, COSM28750, COSM28751,COSM88208, COSM33733, COSM33732, COSM34039, COSM34090, COSM33731,.*P53* gene at TP53_region1, 2,3,4,5,6,7.8 and *ATRX* gene at ATRX_35, ATRX_32, ATRX_31, ATRX_30, ATRX_26, ATRX_22, ATRX_21, ATRX_19, ATRX_18 and ATRX_15. Coverage was 95.05% and target size was 11.81 Kb with 42 targets and 37 amplicons. TERT gene promoter could not be included in panel. The design was constructed using Ion AmpliSeq™ Designer software The NGS was performed and analyzed in 7 cfDNA samples on IonPGM machine as per protocol.

Results: Circulating free DNA levels was significantly higher in cases (712.42±606.52 ng/ml) as compared to healthy controls (88.93±50.38 ng/ml) (p=0.001). Increased cfDNA levels were significantly associated with grade of disease (p=0.0001), age >45 years and presence of p53 mutation. Area under curve in ROC for glioma versus normal controls was 0.79 with sensitivity, specificity and diagnostic accuracy of 79.8%, 100.0% & 82.0% respectively. NGS was carried out in CfDNA in 7 cases. Mutations detected in the cfDNA are detailed in Table 1 and correlated with NGS and IHC studies on tissues. IDH132H non reactive in IHC in an anaplastic oligodendroglioma showed IDH1 mutation at another site

Table 1: Mutational spectrum in cfDNA of ADG by NGS (IonTorrent PGM)

Case	Gene	IHC	CfDNA (ng/ml)	Exon	Type	Amino Acid Change	Coding	Locus	Clinical Significance (FATHMM score
8377	IDH1	R	113.83	Not picked					
	TP53	W		10	SNV	p.Gly334Arg	c.1000G>C	chr17:7574027	Pathogenic (0.99)
1.	ATRX	Ret		18	SNV	p.Asn1633=	c.4899T>C	chrX:76889111	Synonymous
9229	IDH1	NR	710.29	4	SNV	p.Arg132His	c.395G>A	chr2:209113112	Pathogenic (0.94)
2.	TP53	M		5	SNV	p.Pro151Ser	c.451C>T	chr17:7578479	Pathogenic (0.99)
				4	SNV	p.Pro72Arg	c.215C>G	chr17:7579472	Neutral (0.22)
	ATRX	Ret		32	SNV	p.Phe2289Ser	c.6866T>C	chrX:76777850	Missense
				26	SNV	p.Asp2004Glu	c.6012T>A	chrX:76849264	Missense
				9	SNV	p.Pro667Leu	c.2000C>T	chrX:76938748	Neutral 0.39
3628	IDH1	R	60.80	4	SNV	p.Arg132His	c.395G>A	chr2:209113112	Pathogenic (0.97)
3.	IDH2	NA		4	INDEL	p.His175/ MetfsTer74	c.523delC	chr15:90631829	Non pathogenic
	TP53	M		8	SNV	p.Arg273Cys	c.817C>T	chr17:7577121	Pathogenic (0.98)
				5	SNV	p.Leu130Phe	c.388C>T	chr17:7578542	Pathogenic (0.99)
				4	SNV	p.Pro72Arg	c.215C>G	chr17:7579472	Neutral (0.22)
	ATRX	L		22	SNV	p.Pro1829Gln	c.5486C>A	chrX:76872161	Pathogenic (0.99)
				9	SNV	p.Ser856Asn	c.2567G>A	chrX:76938181	Neutral (0.22)
1276	IDH1	R	223.56	4	SNV	p.Arg132His	c.395G>A	chr2:209113112	Pathogenic (0.94)
4.	TP53	M		5	SNV	p.Ala161Thr	c.481G>A	chr17:7578449	Pathogenic (0.91)
	ATRX	Ret.		9	MNV	p.Lys970Thr	c.2909_2910delAGinsCA	chrX:76937838	Missense
8105	IDH1	NR		Not picked					
	TP53	M	1622.24	4	SNV	p.Pro72Arg	c.215C>G	chr17:7579470	Neutral (0.02)
5.	ATRX	Ret.		15	SNV	p.Arg1504=	c.4510C>A	chrX:76907651	Pathogenic (0.75)
7516	IDH1	NR	231.23	4	SNV	p.Arg132Cys	c.394C>T	chr2:209113113	Pathogenic (0.92)
6.	TP53	M		4	SNV	p.Pro72Arg	c.215C>G	chr17:7579470	Neutral (0.02)
	ATRX	Lost		9	SNV	p.Thr668Ile	c.2003C>T	chrX:76938745	Missense
2523	IDH1	NR	10.34	No reads					
	TP53	M							
7.	ATRX	L							

R- Reactive, NR- Non reactive, Ret- Retained, L- Lost, W-Wild, M- Mutated, IHC of IDH1 detects only Arg132His (R132H) mutation

Conclusions: Adult gliomas have significantly high cfDNA levels in sera. NGS allows parallel in depth identification of mutations in cfDNA and may be utilized for inoperable cases and inadequate biopsies. Immunohistochemistry in gliomas is convenient but has the disadvantage of cross reactivity, issues with heterogeneity, incomplete surrogate protein expression in p53 and detection limited to IDH132R mutation for *IDH* gene.

1715 KIAA1549-BRAF Fusion Analysis in Pediatric and Adult Age Groups of Pilocytic Astrocytoma

Jeongwan Kang[1], Jeong Mo Bae[2], Seung-Ki Kim[3], Hongseok Yun[3], Sung-Hye Park[3]
[1]Seoul National University Hospital, Seoul, Korea, Republic of South Korea, [2]Jongno-Gu, SE, Korea, Republic of South Korea, [3]Seoul National University College of Medicine/Hospital, Seoul, Korea, Republic of South Korea

Disclosures: Jeongwan Kang: None; Sung-Hye Park: None

Background: *KIAA1549-BRAF* (B-K) fusion is the most common genetic event in pilocytic astrocytoma (PA) and leads to activation of the mitogen-activated protein kinase (MAPK) signaling pathway.

Design: We retrospectively reviewed 56 cases diagnosed at Seoul National University Hospital (2017-2019), among them 44 cases (26 children under 19-year-old, eight adults more than 18-year-old) with molecular genetic studies included for this study. Molecular genetic studies were carried out with brain tumor-tailored gene panel (BTP) in 22 cases, BRAF gain fluorescence in situ hybridization (FISH) in 23 cases and additional RNA sequencing in one case, which previously could not detect B-K fusion from BTP test.

Results: The overall detection rate of B-K fusion and *BRAF V600E* mutation was 56.8% (25/44) and 6.8%. B-K fusion was found in 64% in children and 25% in adults. The co-occurrence of B-K fusion and *BRAF V600E* mutation was found in 5.6% and 12.5% of pediatric and adult cases, respectively. B-K fusion was detected in 54.2% (13/24) of the posterior fossa (PF) PAs, 75% (6/8) of the 3rd and lateral ventricle PAs, 80.0% (4/5) of optic pathway PAs, 20% (1/5) of cerebral hemisphere PAs and 50% (1/2) of the spinal cord PAs. B-K fusion and *BRAF V600E* mutations were more common in PA of the midline CNS and PF than PA of the cerebral hemispheres (62%: 20%). All 44 patients were alive, but the patients with B-K fusion and BRAF mutations had better progression-free survival than the others. B-K fusion detected by RNA sequencing not by BTP because the fusion site was located in the poor capture area (exon 9) in one case.

Conclusions: We confidently found the B-K fusion by BTP, FISH, and RNA sequencing. This study showed B-K fusion, and *BRAF V600E* mutation was more common in PA of children than PA of adult and PA of the midline and PF than PA of the cerebral hemispheres (62%: 20%). B-K fusion and *BRAF* mutations can be a diagnostic hallmark of PA if the pathological diagnosis is difficult. This study suggested that B-K fusion and *BRAF V600E* mutation might be associated with better progression-free survival. If the fusion site is placed in the poor-capture site of exon 9 of the *BRAF,* RNA sequencing has to be performed.

1716 Ocular Metastases: Histopathological Assessment of 103 Enucleated Eyeballs from Donors with Systemic Malignancy

Afreen Karimkhan[1], Usha Kini[2]
[1]St John's National Academy of Health Sciences, Bengaluru, Karnataka, India, [2]Bangalore, India

Disclosures: Afreen Karimkhan: None; Usha Kini: None

Background: Eye donors from patients with cancers account for 8% of donations but these donor eyes have rarely been availed for transplantation, in view of inconsistent criteria followed for selection of donors with systemic malignancies. Histopathological data from such enucleated donor eyes is scarce. This study is aimed chiefly to assess evidence of metastases in the anterior and posterior segments of the enucleated eyes from donors with systemic malignancy.

Design: Of the 1398 eyes received in a 2-year period at a centralized eye bank, 103 enucleated eyes from 52 patients with systemic malignancy were received for histopathological examination for a detailed study to look for evidence of malignancy. Two calottes were submitted from each eyeball along with middle slab and optic nerve stump. Demographic and histopathological data were correlated.

Results: The donors (n=52) were in the mean age of 61.43 ±14.6 years, with male: female ratio of 1:1. CNS malignancy (12%) was the most common primary followed by leukemia (12%), lymphoma (10%) and the rest were solid organ malignancies. Lung (12%) was the most common metastatic site seen in 52% of donors with systemic metastases.

On gross examination, 103 eyes (1 donor had single functional eye) were near normal. Light microscopy showed conjunctiva, sclera, cornea-limbus, and anterior and posterior chambers with near normal histology. Mononuclear cell infiltrates were noted in periorbital and perioptic nerve adipose tissue(2%), periscleral tissue(4%) and in choroid vessels(4%) from donors with lymphoma, promyelocytic leukemia and glioblastoma multiforme respectively. On further evaluation by Immunohistochemistry, the infiltrates were proved to be reactive B cell lymphoid series and not malignant.

Conclusions: This is one of its kind histopathology study on enucleated eye balls from donors with systemic malignancy; histopathology confirmed near normal ocular structures with no evidence of ocular metastases. Therefore, enucleated eyeballs from donors with systemic malignancy may be considered for corneal as well as limbal stem cell transplantation.

1717 S100-red Staining Enhances Sensitivity of Perineural Invasion Detection in Orbital Squamous Cell Carcinoma

Whayoung Lee[1], Beverly Wang[2], Jeremiah Tao[3], Donald Minckler[4]
[1]University of California Irvine Medical Center, Orange, CA, [2]UC Irvine Medical Center, Orange, CA, [3]UCI Medical Center, Irvine, CA, [4]University of Irvine Medical Center, Orange, CA

Disclosures: Whayoung Lee: None; Beverly Wang: None; Jeremiah Tao: None; Donald Minckler: None

Background: Perineural invasion (PNI) is a process of tumor spread along nerves, an independent prognostic marker of poor outcome. Careful examination of hematoxylin-eosin (H&E) stained slides has been the standard method to detect PNI, but can be problematic even for experienced pathologists. We speculated that S100 red (S100r) might be a useful marker to help identify nerves in squamous cell carcinoma (SCC) specifically in the eyelid or orbit.

Design: We conducted a retrospective data review between January 2010 and December 2018. Orbital exenteration cases and the corresponding reports were reviewed to collect diagnosis, tumor size and presence or absence of documented PNI. The H&E stained slides were reevaluated independently focusing on detecting PNI. S100r staining obtained on the most representative slides of each case were then reexamined and compared to corresponding H&Es to document the presence and number of PNI foci.

Results: Twenty-three orbital exenteration specimens identified counted 30 cases total, including one with two parts. Diagnoses included twenty-seven squamous cell carcinomas, two basosquamous carcinomas, and one midline NUT carcinoma. From the original report, 14 out of 30 cases (46.7%) had been diagnosed as PNI positive, 6 cases PNI negative, 2 cases indeterminate, and the information was not available in 8 reports. Reevaluation of the H&E slides revealed 18 cases (60%) with unequivocal PNI and 3 cases indeterminate for PNI. S100r staining detected PNI in 23 cases (77%) that is five more cases than H&E alone. Seven cases that demonstrated PNI on S100r but not on H&E were due to the small size of the nerve fiber. Two cases that were thought to have PNI turned out to be negative in S100r staining. Not recognizing PNI in these was due either to a very small focus which may have disappeared on a deeper level, or to nerve fiber mimickers, reported as keratin pearls, cautery artifact, and non-neural spindle cells (tumor cells, fibroblasts, and smooth muscle cells).

Conclusions: Unlike other head and neck tumors, no systemized staging is available for the SCC in the orbital area. Reporting accurate PNI status is important because of the rich innervation of the cranial nerves branches and its proximity to the skull base. S100r staining enhances and/or aids the detection of PNI and reduces interpersonal variability. However, the interpretation of the S100r staining should be in conjunction with the H&E slides.

1718 MiR-296-5p Targeting CAD to Block MAPK Signaling Pathway Inhibits the Progression of Glioma

Wencai Li, The First Affiliated Hospital of Zhengzhou University, Zhengzhou, Henan, China

Disclosures: Wencai Li: None

Background: Despite recent advances in the diagnosis and comprehensive treatments of surgery, chemotherapy and radiation therapy, the prognosis for GBM patients remains dismal. High proliferation rate and invasiveness of the tumor are the major obstacles to the management of gliomas, which leads to rapid recurrence or progression. Therefore, it is necessary to explore the molecular mechanism of the initiation and development of glioma has been a research hotspot in the realm of neuro-oncology. Previous studies have found that miR-296-5p played a part in the carcinogenesis of several tumors, but its relationship with glioma is still elusive.

Design: In the current study, the influence of miR-296-5p on the proliferation, colony formation, invasion and migrationability of glioma cells were investigated by cell counting kit-8 (CCK-8), clonogenic, transwell and cell scratch assays. In addition, we used dual luciferase reporter assay and Western blot test to determine whether carbamoyl-phosphate synthetase 2, aspartate transcarbamylase, and dihydroorotase (CAD) is a direct target of miR-296-5p and whether the mitogen-activated protein kinase (MAPK) signaling pathway is a downstream pathway of CAD.

Results: The inhibitory effect of miR-296-5p on the growth of glioma cells was confirmed by in vivo experiments. Also, carbamoyl-phosphate synthetase 2, aspartate transcarbamylase, and dihydroorotase (CAD) is a direct target of miR-296-5p and the mitogen-activated protein kinase (MAPK) signaling pathway is a downstream pathway of CAD. In addition, we revealed that the expression of CAD was an independent prognostic factor in glioma cohorts. Finally, we demonstrate that the inhibitory effects of miR-296-5p on glioma cells was partly reversed by the up-regulation of CAD.

Figure 1 - 1718

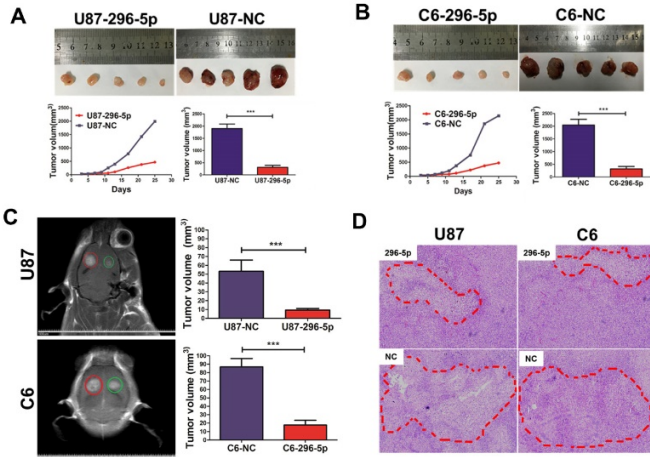

Figure 2 - 1718

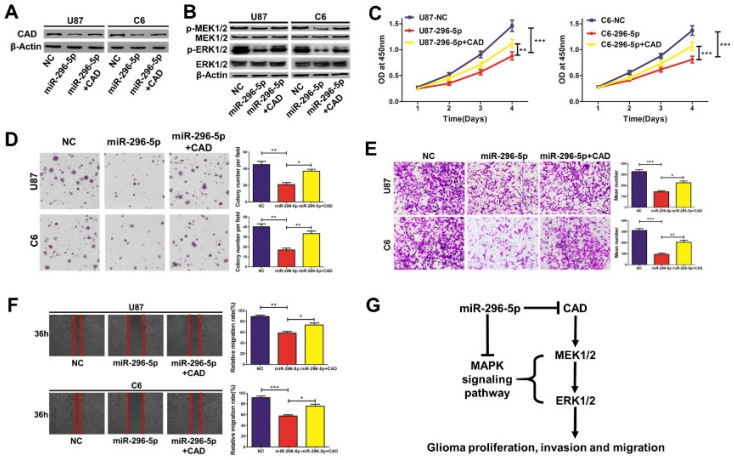

Conclusions: Our data revealed that the miR-296-5p/CAD axis-mediated MAPK pathway was involved in the carcinogenesis of gliomas and has potentialimplications for future treatments against gliomas.

1719 Fine-tuning of Pretrained Convolutional Neural Networks Improves Image Classification Accuracy in Central Nervous System Autopsy Histology

Benjamin Liechty[1], David Pisapia[2], Mert Sabuncu[3]
[1]Weill Cornell Medical College, New York, NY, [2]Weill Cornell Medicine, New York, NY, [3]Cornell University, Ithaca, NY

Disclosures: Benjamin Liechty: None; David Pisapia: None; Mert Sabuncu: None

Background: Convolutional neural networks are a specialized type of deep learning model with applications in computer vision, which learn low-level and high-level image features that might be transferable to new imaging datasets. However, publicly available datasets of histology data are of variable quality, and curation of areas of interest in whole slide scans remains labor intensive, which has limited adoption among pathologists. ImageNet is a publicly available non-specialized dataset used in computer vision, the current version of which contains approximately 14 million natural images curated across approximately 21 thousand indices, and networks pretrained on this dataset have been made publicly available. In this study, we set out to determine whether neural networks pre-trained on non-histologic data from ImageNet can significantly improve classification on subspecialized histology data.

Design: Histologic sections from 19 autopsied brains were photographed at 11 distinct anatomic sites including neocortex (frontal and calcarine), hippocampus, striatum, substantia nigra, pons, medulla, cerebellum, thalamus, spinal cord, and pituitary. Regions were photographed at 4x, 10x, 20x, and 40x objectives, selecting representative fields that could be easily distinguished by a trained neuropathologist. 432 source images were tiled into a series of 256 x 256 pixel images using translational, rotational, scaling, and mirroring transformations for a total set of 2,040,192 tile images. All images from each case were then arbitrarily assigned to either a training set or a validation set, and used to train classifiers based on commonly used convolutional architectures (Inception V3, Xception, and VGG19) initialized with either random weights, or weights obtained from pretraining on ImageNet. 5 iterations of each model were trained on test images until the model stopped improving on validation images. The accuracy of each model was then tested on a random selection of validation images, and compared.

Results:

Architecture	Random initialization		Imagenet initialization	
Inception v3	41.37%	SD 0.82%	71.78%	SD 1.89%
Xception	43.86%	SD 5.08%	71.26%	SD 1.12%
VGG19	44.59%	SD 2.85%	65.96%	SD 4.43%

Table 1. Tile level accuracy by architecture and initialization type.
Note that random chance in this 11-label classification problem is about 9%.

Conclusions: Although the types of images represented in the ImageNet dataset are not representative of histology, the features learned by networks pretrained on this set can be transferred to histology to improve classification accuracy using relatively small datasets of

histology images. This effect was seen in all architectures tested, yielding over 20% improvements in accuracy when compared to randomly initialized networks.

1720 PIK3CA Mutations Identify a Subset of Oligodendrogliomas with Poor Prognosis

Carlos Lopez[1], Antonio Dono[1], Takeshi Takayasu[1], Yoshua Esquenazi[1], Leomar Ballester[1]
[1]*UTHealth McGovern Medical School, Houston, TX*

Disclosures: Carlos Lopez: None; Antonio Dono: None; Takeshi Takayasu: None; Yoshua Esquenazi: None; Leomar Ballester: None

Background: Oligodendrogliomas (ODGs) are infiltrating gliomas representing 2%-5% of all primary brain tumors. According to the 2016 WHO classification, OGDs are defined by the presence of *IDH1/IDH2* mutations and 1p/19q co-deletion. ODGs can be classified based on histology into grade II or III, with grade III tumors having historically worse prognosis. However, the prognostic power of histologic grading in molecularly-defined ODGs remains uncertain. In addition, alterations that correlate with prognosis in ODGs remain to be determined.

Design: We searched our database for patients with ODGs from 2000-2019 and identified 40 cases. All cases were IDH-mutant and 1p/19q co-deleted. Thirty-four cases were analyzed by an NGS assay interrogating at least 236 genes. Age, sex, tumor location, KPS, extent of resection, WHO grade, chemotherapy, radiotherapy, progression, and death, were collected from the EMR. We analyzed Progression Free Survival (PFS) and Overall Survival (OS) in our cases and in TCGA cases using Kaplan-Meier plots. We evaluated the association between genetic alterations and survival using Log-rank test.

Results: The most frequently mutated genes in ODGs were *IDH1/IDH2*, *CIC, TERT*, *NOTCH1* and *FUBP1*. In addition, recurrent mutations in *ALK*, *PIK3CA*, *PIK3R1*, *APC*, *LRP1B, MAP3K1*, *SMARCA4,* and *TSC1* were identified. *PIK3CA* mutations were associated with significantly worse median PFS (21.2 vs. 82.67 months, mutant vs. WT, respectively) and median OS (64.8 vs. 334.1, mutant vs. WT, respectively). Similarly, mutations in *SMARCA4* and *TSC1* were associated with significantly worse OS. We hypothesized that alterations in the *PIK3-ATK-MTOR* pathway might be associated with poor prognosis in OGDs. Our results show that OGDs with mutations in *PICK3CA, PIK3R1,* and *MTOR* have significantly worse PFS and OS. These results are consistent with TCGA database (N=126), showing significantly worse PFS in OGDs with *PIK3-ATK-MTOR* pathway alterations. Interestingly, we did not observe a statistically significant difference in OS in molecularly-defined ODGs based on histologic grade.

Conclusions: Our findings suggest that histologic grading is a suboptimal approach for the stratification of patients with molecularly-defined ODGs. Moreover, alterations in the *PIK3-ATK-MTOR* pathway are associated with worse outcome in these patients. Identification of molecular subgroups of ODGs with worse prognosis is critical and may affect adjuvant therapy strategies.

1721 FOXM1 Immunoreactivity Correlates with Proliferative Index and Clinical Outcome in Meningioma

Calixto-Hope Lucas[1], Stephen Magill[1], Abrar Choudhury[1], Harish Vasudevan[1], Sean Ferris[1], Melike Pekmezci[1], Chetna Gopinath[1], Joanna Phillips[2], Arie Perry[1], David Solomon[1], David Raleigh[2]
[1]*University of California San Francisco, San Francisco, CA,* [2]*University of California San Francisco*

Disclosures: Calixto-Hope Lucas: None; Stephen Magill: None; Abrar Choudhury: None; Sean Ferris: None; Melike Pekmezci: None; Arie Perry: None; David Solomon: None

Background: The molecular drivers of aggressive meningioma are poorly characterized. Beyond NF2, recurrent mutations in meningioma are infrequent. Prior studies have identified Forkhead Box M1 (FOXM1) as a key transcription factor for meningioma proliferation. FOXM1 is a pro-mitotic transcription factor required for cell proliferation during embryonic development and has been implicated in the oncogenesis of various malignancies. FOXM1 has been shown to be enriched in invasive meningioma, and a paradigm in which increased FOXM1 activity cooperates with dysregulated Wnt signaling to drive meningioma proliferation and tumor growth has recently been described.

Design: We utilized an existing integrated meningioma database containing comprehensive clinical data and tissue from 92 meningiomas. The database was enriched for high-grade and recurrent meningiomas (WHO 1 = 41, WHO II = 42, WHO III = 9). Immunohistochemical stains for FOXM1 and Ki-67 (MIB-1) were performed on flash-frozen meningiomas containing >70% tumor cells as determined by H&E staining of frozen sections. The labeling indices (positive nuclei) for both FOXM1 and Ki-67 were averaged across two 200x fields for each individual tumor. Data were dichotomized at the median for outcome analyses according to FOXM1 protein expression (high versus low). The primary endpoint examined was local recurrence or progression. A co-localization immunofluorescence assay for FOXM1 and Ki-67 was also performed on flash-frozen meningioma tissue.

Results: The median length of follow-up was 7.1 years (IQR 2.5-11.4). The median labeling indices in this cohort were 34 nuclei/200x field for FOXM1 (IQR 14-74) and 55 nuclei/200x field for Ki-67 (IQR 23-109). The coefficient of determination (R^2) for FOXM1 and Ki-67 labeling was 0.76. Kaplan-Meier analysis showed a significant difference in local recurrence or progression between the FOXM1-low and FOXM1-high groups (p-value = 0.039). The co-localization immunofluorescence assay showed overlapping expression of FOXM1 and Ki-67 labeling.

Conclusions: Our study further supports FOXM1 as a driver of meningioma proliferation. We show that elevated FOXM1 immunoreactivity is associated with increased cellular proliferation and decreased local control. We also show that FOXM1 and Ki-67 are co-expressed in proliferating cells. The use of FOXM1 immunohistochemistry may provide prognostic value independent of routine grading, to predict outcomes for patients with meningioma.

1722 Associations between FGFR3 Activating Fusions, Molecular Genetic Profiles, and Epigenetic Methylation Signatures in Glioblastomas

Douglas Mata[1], Jamal Benhamida[2], Andrew Lin[3], Philip Jonsson[1], Liliana Villafania[1], Donna Ferguson[1], Ryma Benayed[1], Anita Bowman[4], Alexandra Miller[1], Ingo Mellinghoff[1], Marc Rosenblum[1], Maria Arcila[1], Marc Ladanyi[1], Tejus Bale[1]
[1]Memorial Sloan Kettering Cancer Center, New York, NY, [2]Memorial Sloan Kettering Cancer Center, New York City, NY, [3]New York, NY, [4]Memorial Sloan Kettering Cancer Center, Yeadon, PA

Disclosures: Douglas Mata: None; Jamal Benhamida: None; Andrew Lin: *Grant or Research Support*, Nantomics; *Grant or Research Support*, Bristol-Myers Squibb; Philip Jonsson: None; Liliana Villafania: None; Donna Ferguson: None; Ryma Benayed: None; Anita Bowman: None; Alexandra Miller: None; Ingo Mellinghoff: *Consultant*, Puma Biotechnology, Agios, Debipharm Group; *Speaker*, Roche; *Grant or Research Support*, GE Healthcare, Amgen, Lilly; Marc Rosenblum: None; Maria Arcila: *Speaker*, biocartis; *Speaker*, inviviscribe; Marc Ladanyi: None; Tejus Bale: None

Background: A subset of glioblastomas (GBMs) harbor FGFR3 fusions that constitutively activate its tyrosine-kinase domain (TKD). Molecular features have recently become an important factor in the clinical management of gliomas. Determining whether FGFR3 fusions are associated with other genetic or epigenetic alterations may refine tumor subclassification efforts and impact prognosis and treatment.

Design: Retrospective study of all *FGFR3*-rearranged GBMs diagnosed at this institution between January 2015 and June 2018. A cohort of *FGFR3*-wildtype cases was selected for comparison. Cases were analyzed with an NGS platform that targets up to 468 genes and select introns, as well as with the Infinium MethylationEPIC (850k) platform that assays ~850,000 CpG methylation sites across the genome. Unsupervised hierarchical clustering was performed with the pheatmap package in R.

Results: In all, 680 GBMs underwent NGS. All *FGFR3*-rearranged cases (n = 24; 22 *FGFR3-TACC3*, 1 *ST7L-FGFR3*, and 1 *FGFR3-PTBP1*) and a subset of non-*FGFR3* rearranged cases (n = 37) were selected. The median age at diagnosis was 64.1 years, the median follow-up time was 15.9 months, and 64.6% (40/61) of patients died during follow up. There was no difference in overall survival between patients with or without *FGFR3* fusions (p = 0.30). Of canonical GBM drivers, *FGFR3* fusion-positive cases were less likely to exhibit *EGFR* amplification (4.2% [1/24] vs. 37.8% [14/37], p = 0.002) and more likely to exhibit *FGFR3* amplification (25.0% [6/24] vs. 2.7% [1/37], p = 0.01) (Fig. 1). They were less likely to exhibit *PDGFRA* alterations, although this difference was not statistically significant (4.2% [1/24] vs. 26.1% [8/37], p = 0.08). There was no difference in the frequency of *TERT*, *CDKN2A*/*2B*, *PTEN*, *NF1*, *TP53*, *CDK4*, *MDM2*, *KDR*, *KIT*, *PIK3CA*, or *MDM4* alterations between the groups (p > 0.05). There was no difference in *MGMT* promoter methylation (58.3% [14/24] vs. 62.2% [23/37], p = 0.79). Unsupervised hierarchical clustering showed 2 predominant clusters, 1 of which was enriched with *FGFR3* wild-type tumors (p = 0.04) (Fig. 2).

Figure 1 - 1722

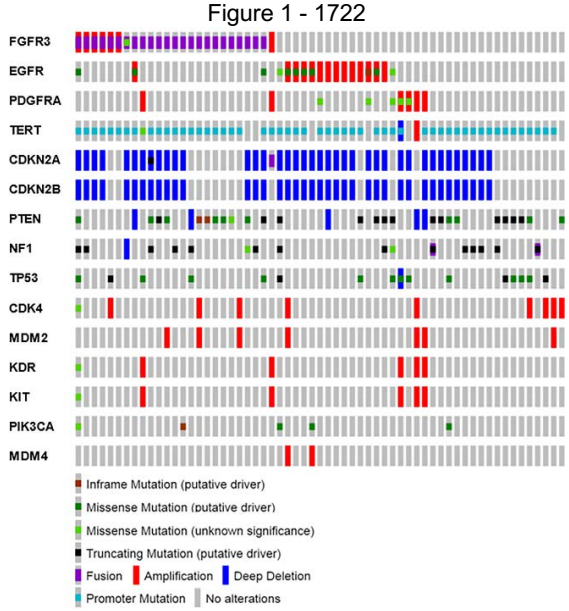

Figure 2 - 1722

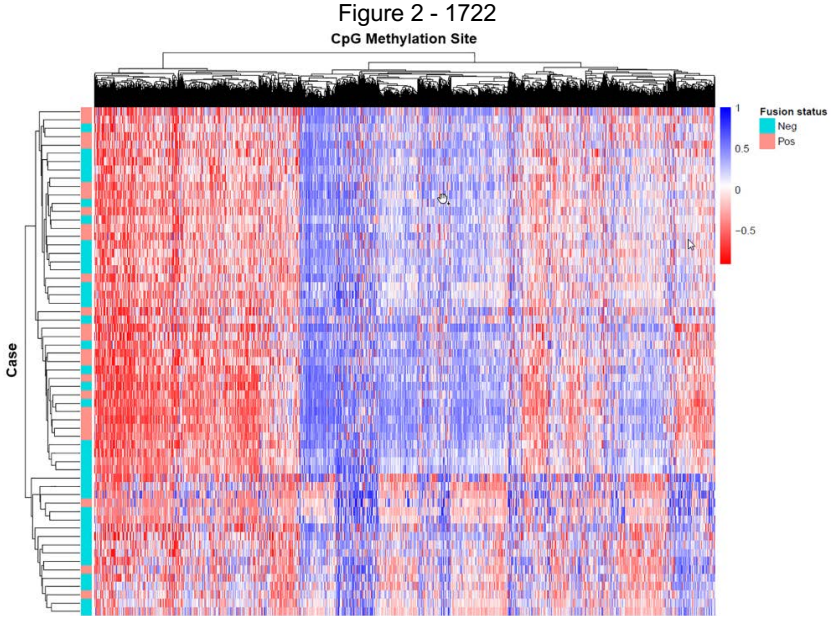

Conclusions: Activating *FGFR3* fusions and *EGFR* amplifications are predominantly mutually exclusive driver events, and a subset of *FGFR3* fusion-positive and -negative GBMs may be divided into distinct methylation-based classes, suggesting differences in tumor biology. Considering ongoing research into therapeutic inhibition of FGFR3 signaling, these differences may affect prognosis and treatment.

1723 Seed-Competent Tau Monomer: a New Biomarker for Tauopathies

Hilda Mirbaha[1], Dailu Chen[2], Lukasz Joachimiak[2], Marc Diamond[2]
[1]UTSW Medical Center, Carrollton, TX, [2]Center for Alzheimer's and Neurodegenerative Diseases, Peter O'Donnell Jr. Brain Institute, University of Texas Southwestern Medical Center, Dallas, TX

Disclosures: Hilda Mirbaha: None

Background: Tau aggregation into ordered assemblies underlies myriad neurodegenerative diseases. We have previously reported that tau monomer exists in two general conformational states. One is inert (M_i) found in normal brains, and the other (M_s) which was purified from brains of tauopathy patients has the capacity to act as conformational templates (seed-competent). However, it has been unclear what is the precise relationship of M_s to pathology as defined either by immunohistochemical abnormalities or development of detergent insoluble aggregates. Moreover, the post-translational modifications (PTMs) that might play a role in the conversion of M_i to M_s have not been elucidated.

Design: We studied a tauopathy mouse (PS19) based on transgenic expression of full-length (1N4R) tau containing a single disease-associated mutation (P301S) to determine when in the disease process Ms first forms. We used established biochemical purification techniques to isolate seed-competent monomer from mice at ages ranging from 0-48 weeks of age. We tested for the presence of Ms using a cellular biosensor system that is based on expression of tau repeat domain (RD) containing two disease-associated mutations (P301L/V337M) fused to cyan and yellow fluorescent protein.

Results: We observed that M_s first appears at 4 weeks of age, months before detergent-insoluble tau becomes apparent. At 4 weeks of age the dominant form of seed-competent tau is a monomer, but within 2 weeks many larger assemblies are detected. Detection of seed-competent monomer was compared with commonly used neurofibrillary tangle staining, AT8, which does not become positive until 3 month of age in PS19 mice. Applying the same method to isolate seed-competent monomer form individuals, would detect the disease when it has just initiated in the brain. We analyzed the pattern of post-translational modification of M_s over this time course. We also purified monomer from brains of 3 Alzheimer's disease patients and 3 control brains. Studying these two datasets revealed a subset of phospho-residues that were unique to M_s.

Conclusions: We propose that formation of seed-competent tau monomer anticipates protein aggregation and immunohistochemical findings. We hypothesize that discrete phosphorylation patterns in tau monomer modulate the strength of long-range contacts and drive conversion of M_i to M_s which in turn modulate local structure. We anticipate that elucidation of the mechanism that promotes this conformational switch will facilitate both therapy and diagnosis.

1724 Neuropathology Decision Support Systems for Resource-Poor Pathologists

Jose Otero[1], Francisco Garagorry[2], Yolanda Cabello-Izquierdo[3], Diana Thomas[1]
[1]The Ohio State University Wexner Medical Center, Dublin, OH, [2]Hospital de Clinicas, Montevideo, Uruguay, [3]The Ohio State University, Columbus, OH

Disclosures: Jose Otero: None; Francisco Garagorry: None; Diana Thomas: None

Background: The advent of molecular sub-typing in primary brain tumors has improved diagnosis of brain cancer patients, but its implementation throughout the world, and even in some parts of the United States, is fraught with caveats. First, in most regions of the world, minimal histopathological infrastructure exists leading to situations where pathologists must incorporate only classical studies, such as H&E staining, with minimal immunohistochemical assays. Middle income countries rarely possess the infrastructure to finance next generation sequencing (NGS) platforms. In the United States, next generation sequencing is rarely performed outside major cancer centers due to lack of insurance reimbursement. Therefore, there is a critical need to develop novel clinical decision support systems capable of aiding pathologists in triaging specimens for specific molecular tests.

Design: A meta-analysis of the Neuropathology literature was performed to identify the proportion of features associated with the diagnostic entities delineated in the 2016 WHO Classification of CNS Tumors. From this meta-analysis, we obtained the distributions of critically important clinical data (age, site, gender), histological features, immunohistochemistry (ki67, IDH1R132H, ATRX, p53, and GFAP), and molecular features (1p19q FISH, 1p19q LOH, EGFR amplification, IDH1/2 sequencing, BRAFV600E mutations). We then constructed a population model in Rstudio containing these diagnostic entities, separated the population into training sets (70%) and test sets (30%), and tested the accuracy of our prediction models using random forest (RF). We also performed cluster analysis using t-SNE.

Results: The t-SNE showed only rare tumor entities well-clustered and distinct from other tumors. Nevertheless, non-linear prediction algorithms were capable of accurately predicting diagnoses. The no information rate for all confusion matrixes was 5.4%. Accuracy using clinical data 34.9%; clinical + histomorphology was 93.4%; clinical + ki67 (no histology) was 73.6%; clinical + histology+ ki67 95.98%; clinical + histology + immunohistochemistry was 96.5%; clinical + histology + immunohistochemistry + 1p19q was 96.5%RF; accuracy using all features was 96.7%.

Conclusions: Despite significant overlap between tumor classes, shallow learning algorithms without molecular features can accurately predict tumor class. These data indicate that such approaches could aid resource-poor pathologists in triaging expensive molecular tests.

1725 Adenovirus KGHV500 Containing Anti-p21Ras scFv Gene Delivered by CIK Cells for the Treatment Therapy of Glioma

Jing Qian[1], Mo Yang[2], Qiang Feng[2], Xinyan Pan[2], Julun Yang[2]
[1]Faculty of Life science and Biotechnology, Kunming University of Science and Technology, Kunming, Yunnan, China, [2]920th Hospital of Joint Logistics Support Force of PLA, Kunming, Yunnan, China

Disclosures: Jing Qian: None; Mo Yang: None; Qiang Feng: None; Xinyan Pan: None; Julun Yang: None

Background: Glioma is the most prevalent type of brain tumors. The efficacy against high-grade gliomas still unsatisfied with currently available therapies. Ras gene, either mutations or overexpression caused by excessive upstream ligand/receptor activity could lead to tumorigenesis in multiple cancers including glioma. We hypothesize that targeting Ras is a reasonable and potential therapy for glioma treatment. Gene therapy delivered by adenovirus (Ads) is a promising trend in the treatment of glioma. The main issue of systemic delivery that clearance and decrease the level of circulating virus particles by neutralizing antibodies could be solved by cell-based drug carrier system. We previously constructed a broad-spectrum anti-p21Ras single-chain variable fragment antibody(scFv) and delivered by Ads KGHV500, where knob has modified to F35, CD46 as its receptor. In this study, we use cytokine-induced killer cells (CIKs) as a secondary carrier to delivery KGHV500 containing the anti-p21Ras scFv gene to investigate the anti-tumor effect of glioma cell line and its xenograft.

Design: Identifying Ras protein and CD46 expression in human glioma cell line U251 by immunohistochemistry (IHC). In vitro, the anti-tumor ability was determined by MTT assay, TUNEL assay, wound healing assay, transwell invasion assay. In vivo, nude-mice glioma tumor xenograft model was constructed, and CIKs was employed to deliver KGHV500 to mice by intravenous injection. The tumors growth volume were drawn, pathological changes and lesions were examined, the expression of p21Ras scFv and virus hexon were detected to evaluate targeting ability and safety.

Results: IHC showed the high expression of p21Ras in the cytoplasm and CD46 expression on the surface of U251 cells. In vitro, the KGHV500 treatment group demonstrated a higher inhibition efficiency on U251 cells migration, invasion, and proliferation, as well as higher apoptosis rate compared with control group. In vivo, tumor volume of the CIK+KGHV500 group was smallest among all groups. Compared with the KGHV500 group, tumor tissue expression of scFv and hexon was higher in CIK+KGHV500 group. The anti-p21Ras scFv was expressed only in the tumor and liver, spleen and kidney in the CIK+KGHV500 group, while those were detected in all tissues except brain in the KGHV500 group.

Conclusions: Our data suggest that KGHV500 and CIK cells as a co-vectors delivering anti-p21Ras scFv enhance the anti-tumor efficacy and safety, and possess a prospect for the treatment of Ras-related cancer.

1726 Genomic and Clinicopathologic Characteristics of Gliomas Harboring Somatic Alteration in NF1 Gene

Somak Roy[1], Abigail Wald[1], Wayne Ernst[1], Yuri Nikiforov[1], Marina Nikiforova[1]
[1]University of Pittsburgh Medical Center, Pittsburgh, PA

Disclosures: Somak Roy: None; Abigail Wald: None; Wayne Ernst: None; Yuri Nikiforov: *Consultant*, Loxo Oncology; Marina Nikiforova: *Consultant*, Loxo Oncology

Background: Gliomas are molecularly heterogeneous tumors across grades and morphologic subtypes. One prior study, using The Cancer Genome Atlas (TCGA) dataset and NF1 FISH analysis, showed that a subset of NF1-altered adult gliomas is associated with a distinct molecular profile and poor prognosis in lower-grade glioma (PMID: 26190195). However, this study and TCGA datasets were enriched with adult patients and WHO grade II-IV gliomas. We analyzed the genomic and clinicopathologic characteristics of NF1-altered gliomas using targeted deep sequencing (GlioSeq® NGS).

Design: After IRB approval, consecutive clinical cases of brain tumors sent for GlioSeq® NGS testing from 2017 to 2019 (23 months), were extracted from our laboratory information system. GlioSeq® is designed to interrogate CNS tumor-related alterations in small stereotactic biopsies and surgically resected tumor samples. It performs targeted sequencing of 30 genes for SNVs and indels, 24 genes for copy number alterations, and 104 genes for fusions.

Results: The genomic and clinicopathologic data were reviewed for a total of 1351 gliomas during a 23 month period. NF1 inactivation via mutation or copy number loss was identified in 162 gliomas (12%). Eight (4.9%) were pediatric and 154 were adult (95.1%) patients. WHO grades I, II, III, and IV gliomas constituted 13 (8%), 6 (3.7%), 23 (14.2%), and 120 (74.1%), respectively. Of the 135 tumors for which location information was available, the majority of the tumors were located supratentorially (102, 75.5%). The most common location was the frontal lobe (52, 51%) in supratentorial tumors, and cerebellum (15/33, 45.5%). NF1 alteration was seen as a primary driver event (101, 62.3%) or secondary event (61, 37.7%) in tumors with alteration in a known driver gene (IDH1, IDH2, EGFR, FGFR3 fusion, H3F3A, SETD2, BRAF, KRAS, and PIK3CA). NF1 inactivation as a sole alteration was seen in 15 cases (9.3%), predominantly in WHO grade I and II tumors. Four tumors (2.5%) demonstrated a hypermutation profile, one of which was in a patient with Lynch syndrome and 3 (1.9%) NF1-mutated gliomas were seen in patients with Neurofibromatosis type 1 syndrome.

Figure 1 - 1726

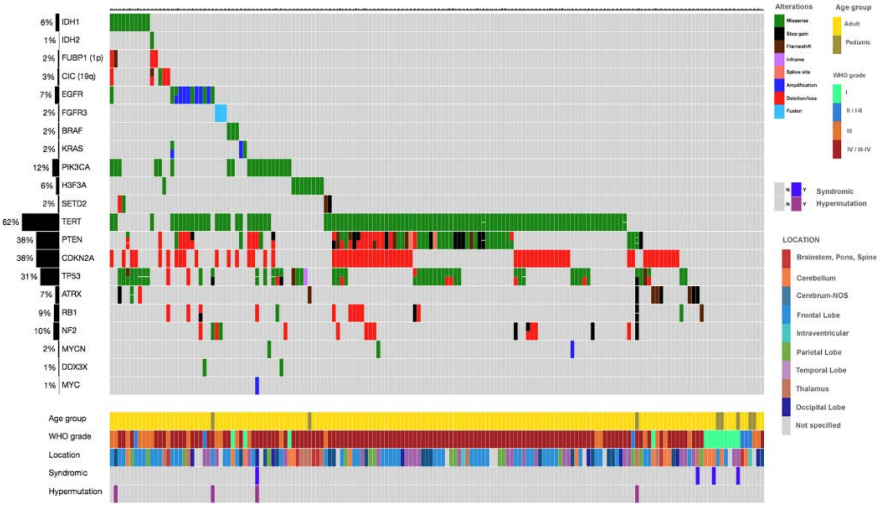

Conclusions: NF1 mutated gliomas are a genetically heterogeneous group of tumors with a distinct molecular and clinicopathologic profile. For accurate diagnostic stratification of NF1-mutated gliomas, the high throughput NGS test results must be evaluated in conjunction with clinical, imaging, neuropathology and medical genetic findings.

1727 Estrogen Receptor is Expressed in Uveal Melanoma: A Potential Target for Therapy

Lynn Schoenfield[1], Sarah Janse[1], David Kline[1], Mary Aronow[2], Arun Singh[3], Caroline Craven[1], Mohamed Abdel-Rahman[4], Colleen Cebulla[4]

[1]The Ohio State University Wexner Medical Center, Columbus, OH, [2]Massachusetts Eye and Ear Infirmary, Harvard Medical School, Boston, MA, [3]Cleveland Clinic, Cleveland, OH, [4]The Ohio State University Wexner Medical Center

Disclosures: Lynn Schoenfield: None; Sarah Janse: None; David Kline: None; Mary Aronow: None

Background: Uveal melanoma (UM) is a rare but deadly cancer, accounting for about 3% of all melanomas. The mortality rate, close to 50% at 15 years, has remained unchanged for decades. There are no published reports documenting the presence of estrogen receptor (ER) in UM. However, newer and more robust methods for studying ER expression in breast cancer yet to be applied to UM. Gender-based differences in survival provide additional rationale for evaluating potential hormonal driven mechanisms in UM. For example, the RARECARE project in which 4097 cases of uveal melanoma were evaluated found that five-year survival rates were better for women than for men, and another recent study reported differences in incidence and metastasis-related mortality by gender, with males having a worse prognosis.

Design: Immunohistochemical analyses for ER were performed on two cohorts, one at the Cleveland Clinic and the second at The Ohio State University Wexner Medical Center. The findings were correlated with clinical features and molecular studies where available. ER was considered positive if, as in breast carcinoma, greater than 1% of tumor nuclei were positive.

Results: In the initial cohort, 59% of 34 cases ER (+). Males and females showed similar results (n=9 and 11, respectively), while most ER (-) tumors were from males (n=12 males, 2 females). If male and ER (+), 5/8 (63%) died from disease or had metastases compared to 3/12 (25%) if male and ER (-). If female and ER (+), 5/12 (42%) died from disease or had metastases compared to 0/2 (0%) if female and ER (-). The second cohort had a similar percentage of ER (+) UM cases (62% of 55 cases from 47 patients). The quantitative levels of ER expression were categorized as negative (<1%), found in 38%, low positive (1-9%), found in 28%, and positive (≥10%), found in 34% of cases. The second cohort had 5 matched pairs (primary and metastasis), and concordance of ER staining was found in 4 of the 5

patients. Kaplan-Meier survival curves on the second cohort revealed no statistically significant difference in probability of surviving without metastasis between ER (+) and ER(-). However, it was noted in the OSUWMC cohort that ER (+) tumors were more likely to be associated with monosomy 3/8q gain and/or class 2 status by gene expression profiling, known poor prognostic indicators.

Table 1: OSUWMC cohort, Patient Characteristics, 47 patients with adequate tissue

Variable	Level	Total (n=47)
ER Status	Positive	29 (62%)
	Negative	18 (38%)
Sex	Female	19 (40%)
	Male	28 (60%)
Age (years)	Mean (SD) (min, max)	60 (16.5) (17, 87)
Metastasis	No	27 (57%)
	Yes	20 (43%)
Death	No	33 (70%)
	Yes, due to disease	12 (26%)
	Yes, due to competing cause	2 (4%)
Metastasis or death due to disease	Missing	1 (2%)
	Yes	27 (57%)
	No	19 (40%)

Figure 1 - 1727

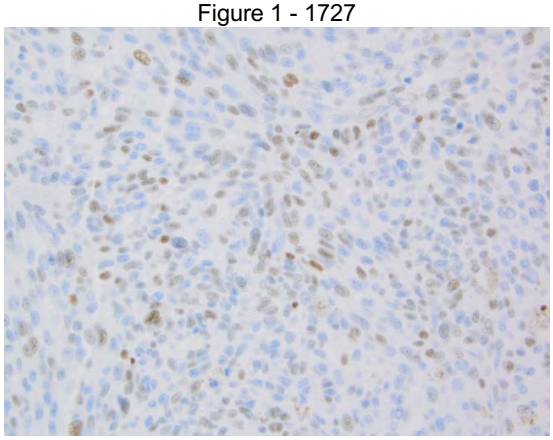

Conclusions: The authors conclude that ER is positive in more than half of UM tumors, both primary and metastatic raising the possibility of targeted therapy.

1728 Does Grade III Astrocytoma Exist?

Ashley Scholl[1], Francisco Franyutti[2], Rudolph Castellani[3]
[1]West Virginia University Health Sciences Center, Charleston, WV, [2]West Virginia University Health Sciences Center, Philippi, WV, [3]West Virginia University Health Sciences Center, Morgantown, WV

Disclosures: Ashley Scholl: None; Francisco Franyutti: None; Rudolph Castellani: None

Background: Grading of astrocytomas at present is morphological, despite the integrated approach to the overall interpretation according to the WHO 2016 recommendations. Mitotic activity is particularly pivotal in distinguishing low grade from high grade astrocytomas, indicating a thin and somewhat subjective line between lesions that are viewed as biologically distinct. IDH mutation analysis, however, adds prognostic information. We hypothesized that IDH status may super-cede traditional indices of tumor grade in astrocytomas.

Design: To address this hypothesis, we examined 91 consecutive diffuse astrocytomas. Data included demographics, clinical data, imaging outcomes, WHO grade, and molecular status (IDH, 1p/19q, MGMT). IDH-1 (R132H) immunohistochemistry and/or next generation sequencing was used in all cases. 1p/19q was assessed by FISH. Co-deleted tumors were excluded from the analysis. MGMT promoter methylation was performed by methylation-specific RT-PCR. This study was approved by the WVU institutional review board.

Results: Of the 91 cases analyzed at the time of submission (70 additional cases will be analyzed), 10 were IDH-mutant non-GBM diffuse astrocytomas (4 grade II, 6 grade III). All but one were alive at follow up (mean survival to date 30.9 +/- 15.2 months). 6 IDH wild-type non-

GBM diffuse astrocytomas were identified, with 5 dying of disease (mean survival 12.8 +/- 6.7 months) (P < 0.02, student t-test). The difference was significant despite all but one IDH-mutant patient being alive at follow up. 51 IDH-wildtype glioblastomas were identified with an average survival of 14.9 months; 21 of 51 alive at follow up (range 4 - 42 months). 6 IDH-mutant glioblastomas were identified, with varying outcome. In this initial series, the favorable survival among IDH-mutant versus IDH-wildtype astrocytomas was irrespective of imaging findings, MGMT promoter methylation status, and treatment.

Conclusions: In this study, we found that there was no prognostic value in the WHO grade III astrocytoma category, since the behavior of IDH-mutant WHO grade III astrocytomas are in line with the traditional notion of WHO grade II astrocytomas, and IDH-wildtype WHO grade III astrocytomas approach the behavior of glioblastoma. Thus the artificial separation of grade II from grade III astrocytoma by mitotic activity, or grade III from grade IV by secondary host responses (necrosis, microvascular proliferation), might be reconsidered or even discarded in light of IDH status.

1729 Clinicopathologic Features and Genomic Landscape of NF1-Associated Gliomas

Emily Sloan[1], Jeffrey Hofmann[2], Cathryn Cadwell[1], Julieann Lee[1], Melike Pekmezci[1], Tarik Tihan[1], Andrew Bollen[3], Alyssa Reddy[1], Arie Perry[1], David Solomon[1]
[1]University of California San Francisco, San Francisco, CA, [2]University of California San Francisco Pathology, San Francisco, CA, [3]University of California San Francisco School of Medicine, Kentfield, CA

Disclosures: Emily Sloan: None; Jeffrey Hofmann: None; Cathryn Cadwell: None; Julieann Lee: None; Melike Pekmezci: None; Tarik Tihan: None; Andrew Bollen: None; Alyssa Reddy: None; Arie Perry: None; David Solomon: None

Background: Neurofibromatosis type 1 (NF1) is an autosomal dominant tumor predisposition syndrome caused by germline inactivation of the *NF1* tumor suppressor gene. Here we comprehensively evaluate the clinical, radiologic, histologic, and genetic features of NF1-associated gliomas occurring in both children and adults.

Design: The study cohort was composed of 16 NF1 patients diagnosed by clinical criteria and/or germline sequencing who underwent resection of primary glial neoplasms. Clinical, radiologic, and histologic features were correlated with the results of targeted next-generation sequencing.

Results: The 8 male and 8 female patients ranged from 1 to 58 years of age at time of surgery. Histologic evaluation demonstrated 9 low-grade gliomas (6 pilocytic astrocytomas, 2 gangliogliomas, 1 low-grade astrocytoma NOS), and 7 high-grade gliomas (3 anaplastic pilocytic astrocytomas, 3 high-grade astrocytomas NOS including one with a primitive neuronal component, and 1 H3 K27M-mutant diffuse midline glioma). All tumors were found to harbor biallelic inactivation of *NF1*, due to a heterozygous germline mutation accompanied by either somatic loss of heterozygosity or a somatic mutation affecting the remaining wildtype allele. In 8 of the 9 low-grade gliomas, biallelic *NF1* inactivation was the solitary pathogenic alteration identified, while the remaining tumor had a frameshift mutation in *ZBTB20*. In contrast, all of the 7 high-grade gliomas harbored additional pathogenic alterations beyond NF1 inactivation. These included *CDKN2A/B* homozygous deletion (n=4); mutations of *ATRX* (3), *TP53* (2), *PIK3CA* (1), *HIST1H3B* p.K27M (1), and *PPM1D* (1); and amplifications of *CDK4* (1) and *MYCN* (1).

Conclusions: NF1-associated gliomas encompass a broad histologic spectrum that are molecularly unified by the presence of bialleleic inactivation of *NF1*. Low-grade tumors mostly harbor solitary *NF1* inactivation, while high-grade tumors are characterized by additional pathogenic alterations, many of which are also commonly found in sporadic high-grade gliomas. These results suggest that NF1-associated gliomas can be divided into low- and high-grade molecular subgroups based on the presence or absence of additional accompanying genetic alterations. Future studies should incorporate molecular characterization with clinical outcomes to further define the potential prognostic significance of NF1-associated glioma subgroups.

1730 Clinical Significance of Histone Deacetylase-2 Expression in Uveal Melanoma

Stamatios Theocharis[1], Georgia Levidou[2], Pawel Gajdzis[3], Christos Masaoutis[2], Piotr Donizy[4], Eugene Danas[5], Samer Albesher[2], Penelope Korkolopoulou[6], Jerzy Klijanienko[7]
[1]National and Kapodistrian University of Athens, Medical School, Athens, Greece, [2]First Department of Pathology, Medical School, National and Kapodistrian University of Athens, Athens, Attica Greece, Greece, [3]Department of Pathomorphology and Oncological Cytology, Wroclaw Medical University, Wroclaw, Dolnoslaskie, Poland, [4]Wroclaw Medical University, Wroclaw, Poland, [5]University of Athens, Athens, Greece, [6]Medical School, National and Kapodistrian University of Athens, Athens, Attica, Greece, [7]Department of Pathology, Institut Curie, Paris, France, Paris, France

Disclosures: Stamatios Theocharis: None; Georgia Levidou: None; Pawel Gajdzis: None; Christos Masaoutis: None; Piotr Donizy: None; Penelope Korkolopoulou: None; Jerzy Klijanienko: None

Background: Uveal melanoma (UM) represents the most common primary intraocular malignancy in adults with high metastatic potential and poor prognosis. Histone Deacetylases (HDACs), through post-translational histone modifications and subsequent gene expression alterations, play a key role in carcinogenesis. Aim of this study was to evaluate the clinical significance of HDAC-2 expression in UM.

Design: HDAC-2 expression [percentage and intensity of staining as categorical variables, and their product IRS (classified into 4 levels: negative, mild, moderate and strong)] was assessed immunohistochemically in 74 UM tissue specimens and was correlated-with tumours' clinicopathological characteristics, presence of tumour infiltrating lymphocytes (TILS) and with patients' overall (OS) and disease free survival (DFS). The observed heterogeneous pattern of HDAC-2 immunostaining (classified into isolated clusters of tumour cells, multiple clusters and widespread expression throughout the tumour) was also correlated with the above mentioned variables.

Results: UM patients with negative/mild nuclear HDAC-2 IRS were older than those with moderate/strong IRS (p=0.05), whereas tumour size significantly differed among the four levels of nuclear HDAC-2 IRS (p=0.0132). HDAC-2 nuclear IRS varied significantly among cases with different histological types, being higher in the epithelioid one (p=0.034). HDAC-2 nuclear IRS was frequently higher in cases presenting "brisk" TILS (p=0.037). In survival analysis HDAC-2 nuclear IRS was correlated with longer patients' OS (p=0.0415), a result which remained significant in multivariate analysis after adjustment for established UM prognosticators (p=0.001). The heterogeneous pattern of HDAC-2 nuclear staining showing isolated clusters of tumour cells was also correlated with longer patients' OS (p=0.0012). A correlation between either HDAC-2 nuclear IRS or heterogeneous pattern of HDAC-2 nuclear staining and DFS was not observed.

Conclusions: HDAC-2 expression is considered as an independent favourable prognostic factor in UM patients.

1731 STAT3 Expression is Associated with NAB2-STAT6 Fusion Gene in Solitary Fibrous Tumors of the Central Nervous System

Sufang Tian[1], Li Niu[2]
[1]Wuhan University Zhongnan Hospital, Los Angeles, CA, [2]Department of Pathology, Zhongnan Hospital of Wuhan University, Wuhan, Hubei, China

Disclosures: Sufang Tian: None; Li Niu: None

Background: Solitary fibrous tumor (SFT) is a fibroblastic mesenchymal neoplasm characterized by a prominent branching vascular pattern. It arises in different sites such as soft tissue, pleura, visceral organs and rarely in the central nervous system (CNS). SFT and hemangiopericytomas (HPC) are now classified as a histological spectrum containing the fusion of the NAB2 and STAT6 genes, which act as a driver mutation that activates the STAT3-EGR1 pathway. STAT6 is a transcription factor of the STAT family used as a diagnostic marker for SFT/HPC, while the role of STAT3 in SFT/HPC of the CNS is still unknown. This study was sought to investigate STAT3 expression and its association with clinical behavior of SFT/HPC tumors in the CNS.

Design: Twenty two SFT/HPC cases of CNS diagnosed at Zhongnan Hospital of Wuhan University from 2016 to 2019 were selected. Data from tissue chip immunohistochemistry staining for STAT3, STAT6, ki67 and survival were analyzed. The dilution ratio of anti-STAT3 antibody from ZEN-BIO company was 1:100 and immunostaining procedure was followed the standard protocol.

Results: Expression of STAT3 was detected in all of the CNS SFT/HPC tumor cases. In addition, overexpression of STAT3 was associated with higher grade and worse prognosis.

Figure 1 - 1731

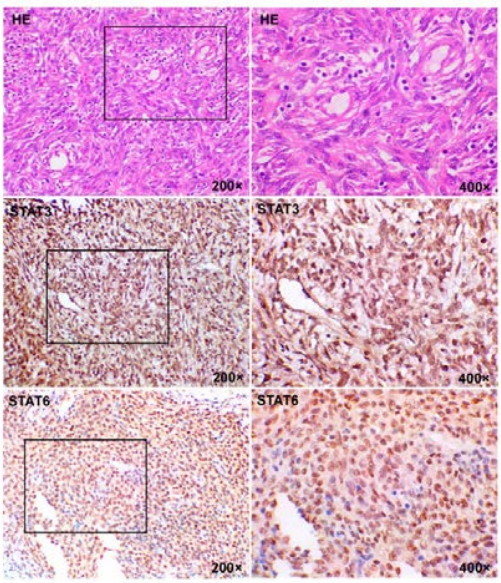

Conclusions: The nuclear entry of STAT6 in SFT/HPC tumors resulting from the NAB2-STAT6 fusion drives the neoplastic transformation. STAT3 contributes to the malignancy of the SFT/HPC tumors in the CNS. It is suggested that the resulting activation of the STAT pathway in CNS SFT/HPC tumors may act as a predictive marker of malignancy and STAT3 can be a promising therapeutic target for CNS SFT/HPC tumors.

1732 Clinicopathologic and Molecular Features of Gliomas Harboring NTRK Fusions

Matthew Torre[1], David Meredith[2], Mariarita Santi[3], Sonika Dahiya[4], Azra Ligon[5], Shakti Ramkissoon[6], Jonathan Serrano[7], Michael DeLorenzo[8], Matija Snuderl[7], Sanda Alexandrescu[9]
[1]Brigham and Women's Hospital, Harvard Medical School, Brookline, MA, [2]Boston, MA, [3]The Children's Hospital of Philadelphia, Washington, DC, [4]Washington University in St. Louis, St. Louis, MO, [5]Brigham and Women's Hospital, Boston, MA, [6]Foundation Medicine, Inc., Morrisville, NC, [7]New York University, New York, NY, [8]New York University, New York City, NY, [9]Boston Children's Hospital, Harvard Medical School, Boston, MA

Disclosures: Matthew Torre: None; David Meredith: None; David Meredith: None; Mariarita Santi: None; Sonika Dahiya: None; Azra Ligon: None; Shakti Ramkissoon: *Employee*, Foundation Medicine/Roche; Jonathan Serrano: None; Michael DeLorenzo: None; Matija Snuderl: None; Sanda Alexandrescu: None

Background: *NTRK* fusions are seen in a range of tumors and are thought to drive tumorigenesis through constitutive activation of the MAPK and PI3K/AKT pathways. Large scale genetic sequencing studies have shown that *NTRK* fusions are present in a subset of gliomas but may be exceptionally rare depending on age group and location. Demonstrating the presence of an *NTRK* fusion has significant clinical implications, as these tumors may respond to selective kinase inhibitor therapy. In this multi-institutional study, we describe the clinicopathologic characteristics and molecular aberrations of *NTRK*-fused gliomas.

Design: With institutional review board approval, the demographics, clinical history, radiology, and pathology slides were reviewed for 14 patients with confirmed *NTRK* fusions. Routine histology, immunohistochemistry, DNA microarray analysis, targeted exome sequencing, RNA-based fusion detection, and genome-wide methylation profiling were performed on FFPE tissue.

Results: The median age at time of diagnosis was 22 years (range 3 months to 54 years), and there was a female predominance (10 F, 4 M). 11/14 of the tumors were hemispheric, two arose in the posterior fossa, and one involved the 3rd ventricle. *NTRK3-ETV6* fusions were observed in 2 cases, but all other fusion partners were unique. *NTRK2* fusions were more prevalent in pediatric tumors, while adult tumors showed frequent fusions in *NTRK1/3*. Most tumors demonstrated an infiltrative pattern of growth, and there was striking intertumoral heterogeneity, with histology ranging from low to high grade. Subsets of cases contained calcifications, microvascular proliferation, necrosis, and morphologies reminiscent of oligodendroglioma, ganglioglioma, and pleomorphic xanthoastrocytoma. The most common copy number alterations were polysomy 7 and loss of *CDKN2A/B*, irrespective of histologic grade. All adult cases had high grade histology, with a proportion of cases containing point mutations involving *TP53*, *PTEN*, *ATRX*, or the *TERT* promoter; one had *IDH1(R132H)* mutation. Methylation profiling with DKFZ classification analysis matched one case to anaplastic PXA and another case to infantile hemispheric glioma, but otherwise NTRK-fused gliomas matched poorly or not at all to known methylation classes. NTRK-fused gliomas may be associated with poor clinical prognosis.

Conclusions: *NTRK*-fused gliomas are histologically and molecularly heterogenous. Their identification is clinically important in the era of targeted selective kinase inhibitor therapy.

1733 Abstract Withdrawn

1734 Care Setting Disparities in 1p/19q Codeletion Testing Rates for Diffuse Gliomas

Matthew Torre[1], Nayan Lamba[2], Sneha Gupta[3], Timothy Smith[4], J. Bryan Iorgulescu[5]
[1]Brigham and Women's Hospital, Harvard Medical School, Brookline, MA, [2]Brigham and Women's Hospital and Harvard Medical, Boston, MA, [3]Brigham and Women's Hospital, Morgantown, WV, [4]Brigham and Women's Hospital, Harvard Medical School, Boston, MA, [5]Boston, MA

Disclosures: Matthew Torre: None; Sneha Gupta: None; J. Bryan Iorgulescu: None

Background: Chromosomal 1p/19q codeletion testing is an essential component of diagnostic work-up for diffuse gliomas. However, socioeconomic barriers to appropriate testing are unknown.

Design: All newly-diagnosed diffuse glioma patients with oligodendrocytic, mixed, or unclear histology were identified from the National Cancer Database (>70% of all newly-diagnosed cancers in the US) from 2010-2016. Multivariable logistic regression was utilized to understand socioeconomic factors associated with 1p/19q codeletion testing.

Results: 5,962 newly-diagnosed diffuse glioma patients with oligodendrocytic (3,608), mixed (1,615), and unclear (739) histologies had data about 1p/19q codeletion testing encoded; of which 76%, 34%, and 19% were 1p/19q-codeleted respectively.

In multivariable logistic regression, elderly patients and patients diagnosed at community cancer programs (compared to academic/research hospitals) were significantly less likely to be tested (Table 1). Gliomas with mixed or unclear histology were significantly less likely to be tested than those with oligodendrocytic histology. Testing patterns also differed by geographic location. Patient's race/ethnicity, sex, insurance status and tumor grade did not impact testing rates. Rates of 1p/19q-codeletion testing have risen from 57% of cases in 2010 to 78% in 2016 ($p<0.001$).

		Multivar logistic regression for having 1p/19q codeletion testing		
		OR	**95%CI**	**p-val**
Age at Diagnosis (yr)				
	<40	0.75	(0.49-1.14)	0.18
	40-49	1.03	(0.83-1.27)	0.80
	50-59		Reference	
	60-69	0.99	(0.76-1.29)	0.95
	70+	0.64	(0.45-0.92)	0.02
Sex				
	Male		Reference	
	Female	1.00	(0.88-1.14)	1.00
Race/Ethnicity				
	White		Reference	
	Black	0.76	(0.57-1)	0.05
	Asian/Pacific islander	0.75	(0.53-1.07)	0.12
	Hispanic	0.81	(0.63-1.04)	0.10
	Other/Unknown	1.14	(0.7-1.87)	0.60
Insurance Status				
	Not Insured		Reference	
	Private Insurance/Managed Care	1.27	(0.97-1.66)	0.08
	Medicaid	1.10	(0.81-1.51)	0.53
	Medicare	1.12	(0.78-1.61)	0.53
	Other Government	1.15	(0.68-1.94)	0.61
	Insurance Status Unknown	0.64	(0.36-1.13)	0.12
Median income of patient's ZIP code				
	< $38,000	0.93	(0.75-1.15)	0.52
	$38,000-$47,999	1.00	(0.83-1.2)	0.98
	$48,000-$62,999	0.83	(0.71-0.98)	0.03
	>=$63,000		Reference	
Hospital Type				
	Community Cancer Program	0.56	(0.35-0.9)	0.02
	Comprehensive Community Cancer Program	0.98	(0.79-1.22)	0.88
	Academic/Research Program		Reference	
	Integrated Network Cancer Program	1.13	(0.86-1.47)	0.37
	Suppressed due to <40yo		(omitted)	
Hospital Location				
	New England	0.81	(0.48-1.36)	0.42

	Middle Atlantic	0.66	(0.42-1.02)	0.06
	South Atlantic	0.50	(0.33-0.77)	<0.001
	East North Central	0.91	(0.59-1.39)	0.65
	East South Central	0.73	(0.43-1.25)	0.25
	West North Central	1.00	(0.63-1.6)	0.99
	West South Central	0.58	(0.36-0.94)	0.03
	Mountain		Reference	
	Pacific	0.89	(0.57-1.39)	0.61
	Suppressed due to <40yo		(omitted)	
Year of Diagnosis				
	2010	0.28	(0.22-0.36)	<0.001
	2011	0.56	(0.43-0.74)	<0.001
	2012	0.59	(0.45-0.77)	<0.001
	2013	0.72	(0.55-0.94)	0.02
	2014	0.81	(0.62-1.07)	0.14
	2015	0.75	(0.57-0.99)	0.04
	2016		Reference	
Histology				
	Oligodendrocytic		Reference	
	Mixed	0.86	(0.74-1)	0.05
	Unclear	0.19	(0.15-0.24)	<0.001
Grade				
	Low		Reference	
	High	0.99	(0.86-1.13)	0.88

Conclusions: Although 1p/19q codeletion testing rates for diffuse gliomas have been increasing, there remains approximately 20%, 25%, and 65% of newly-diagnosed cases with oligodendrocytic, mixed, or unclear histology that do not undergo testing within the first year following diagnosis. Patient characteristics like insurance status and race/ethnicity no longer appear to be significant barriers to appropriate 1p/19q codeletion testing. Notably, patients treated at community cancer programs were significantly less likely to undergo testing; suggesting the opportunity for improving diagnostic standard-of-care across different care settings.

1735 The RANK Pathway in Breast Cancer Metastatic to the Brain

Kai Wang[1], James Hackney[2], Gene Siegal[2], Shi Wei[2]
[1]University of Florida, Gainesville, FL, [2]The University of Alabama at Birmingham, Birmingham, AL

Disclosures: Kai Wang: None; James Hackney: None; Gene Siegal: None; Shi Wei: None

Background: Receptor activator of nuclear factor-kB (RANK) and its ligand, RANKL, are essential for mammary gland development and play a vital role in breast carcinogenesis in mouse models. The RANKL/RANK signaling also drives thermoregulation and modulates the inflammatory activation of microglial cells in the brain. We have previously shown that the expression of RANKL in primary breast cancer (BC) was negatively associated with brain metastases, while significantly higher levels of RANK were seen in BC with brain metastases. In this study, we sought to examine the expression of RANK and RANKL in metastatic BC to the brain.

Design: A total of 40 cases of metastatic BC to the brain with sufficient tumoral tissue and non-necrotizing stroma were identified, including all three major BC subtypes (14 luminal, 14 HER2, and 12 TNBC). Ten normal brains obtained during autopsy were also included as controls. Protein expression was evaluated by immunohistochemistry using a H-score determined by multiplying the intensity by the percentage of positive staining.

Results: RANK was variably expressed in metastatic BC (mean H-score 140; range 0-280) but was minimally expressed in the adjacent brain parenchyma (mean H-score 29). In contrast, the expression of RANKL was minimal in metastatic BC (mean score 14) but highly

variable in tumoral stroma (mean H-score 154; range 10-300; *P*<.0001). RANKL expression in normal brain stroma was negligible (mean H-score 7; *P*<.0001). Histologic grade and BC subtypes were not significantly associated with RANK expression in metastatic BC. A higher level of RANKL in stroma was found in association with TNBC (mean H-score 189) when compared to luminal (mean H-score 136) and HER2 (mean H-score 142) subtypes but did not reach statistical significance. Interestingly, a significant negative correlation between RANK in metastatic BC and RANKL in tumoral stroma was identified (R^2=0.351; *P*<.0001).

Conclusions: RANK is frequently expressed by primary tumors while RANKL is often detected in the tumor microenvironment and together they participate in cancer development. Our findings suggest that the same principle may apply to distant sites. A potential mechanism for brain metastasis is that the retention of RANK and reduced RANKL in primary and metastatic BC would allow RANK to interact with the RANKL present in the cells at the site of metastasis. Further investigation of the soluble form of RANKL, being more active after shedding, may provide further insight into brain metastasis.

1736 Association of Hippocampal Sclerosis, TDP-43 Proteinopathy, and Cerebral Microvascular Disease in Advanced Age

Shih-Hsiu Wang[1], William Harrison[2], John Ervin[3], Beiyu Liu[3], Cindy Green[3]
[1]Department of Pathology, Duke University School of Medicine, Durham, NC, [2]Wake Forest Baptist Medical Center, Clemmons, NC, [3]Duke University Medical Center, Durham, NC

Disclosures: Shih-Hsiu Wang: None; William Harrison: None; John Ervin: None; Cindy Green: None

Background: Hippocampal sclerosis (HS), TDP-43 proteinopathy, and cerebral microvascular disease have been observed with increased frequency in individuals of advanced age, and association between these pathologies have been described in previous reports, suggesting a common pathogenic mechanism. However, the association between microvascular disease and TDP-43 proteinopathy was not replicated in some recent studies. In this study, we analyzed the brains of individuals over 90 years of age from the Duke Kathleen Price Bryan Brain Bank to establish the prevalence of different pathologies and explore the association between HS, TDP-43 proteinopathy, and arteriolosclerosis.

Design: 50 subjects aged 90 years or older were selected for our cohort based on availability of neurocognitive data. A semi-quantitative assessment for TDP-43 positive inclusions and neurites was performed in the amygdala, hippocampus with entorhinal and inferior temporal cortices, and frontal lobe, and given a score of sparse (1-2 inclusions or neurites/400X field), moderate (3-5 inclusions or neurites/400X field), or frequent (> 6 inclusions or neurites/400X field). Assessment of Alzheimer's disease (AD) pathology, Lewy body pathology, HS, and arteriolosclerosis were performed according to published guidelines. Chi-squared test/Fisher's exact tests were performed to test the association between pathologies. A multinomial logistic regression model was fit to examine the association of dementia with different pathologies.

Results: The prevalence of HS is 22%, TDP-43 proteinopathy is 42%, and arteriolosclerosis ranges from 58% in the frontal lobe, 70% in the hippocampus and amygdala, and 90% in the basal ganglia in our cohort. There is significant association between HS and TDP-43 proteinopathy ($p<0.05$), but not AD neuropathologic change or other pathologies. There is also significant association between TDP-43 proteinopathy and arteriolosclerosis in the amygdala ($p<0.05$) and frontal lobe<($p<0.01$). By logistical regression, the level of AD neuropathologic change has the strongest effect on the odds of having dementia, while other pathologies, including HS and TDP-43 proteinopathy show a moderate effect.

Table 1 : HS and ADNPC by TDP-43				
	TDP-43			
	No (N=29)	Yes (N=21)	Total (N=50)	p value
HS				0.0356[1]
No	26 (89.7%)	13 (61.9%)	39 (78.0%)	
Yes	3 (10.3%)	8 (38.1%)	11 (22.0%)	
ADNPC				0.4118[1]
High	1 (3.4%)	3 (14.3%)	4 (8.0%)	
Intermediate	15 (51.7%)	8 (38.1%)	23 (46.0%)	
Low	11 (37.9%)	7 (33.3%)	18 (36.0%)	
None	2 (6.9%)	3 (14.3%)	5 (10.0%)	
[1]Fisher Exact				

Table 2: Microvascular Disease by TDP-43				
	TDP-43			
	No (N=29)	Yes (N=21)	Total (N=50)	p value
Arteriolosclerosis in Amygdala				0.0113[1]
No	13 (44.8%)	2 (9.5%)	15 (30.0%)	
Yes	16 (55.2%)	19 (90.5%)	35 (70.0%)	
Arteriolosclerosis in Hippocampus				0.0606[1]
No	12 (41.4%)	3 (14.3%)	15 (30.0%)	
Yes	17 (58.6%)	18 (85.7%)	35 (70.0%)	
Arteriolosclerosis in Frontal Lobe				0.0012[1]
No	18 (62.1%)	3 (14.3%)	21 (42.0%)	
Yes	11 (37.9%)	18 (85.7%)	29 (58.0%)	
Arteriolosclerosis in Basal Ganglia				0.0657[1]
No	5 (17.2%)	0 (0.0%)	5 (10.0%)	
Yes	24 (82.8%)	21 (100.0%)	45 (90.0%)	
[1]Fisher Exact				

Conclusions: The results of this study show a significant association between arteriolosclerosis, TDP-43 proteinopathy, and HS in our cohort of individuals 90 years or older. Further studies are underway to investigate the pathogenic mechanism that connect these different pathologies.

1737 Molecular Subgroups of Medulloblastoma based on NanoString Assay: A Large Sample Size Clinical Research in Chinese Population

Weiwei Wang, The First Affiliated Hospital of Zhengzhou University, Zhengzhou, Henan, China

Disclosures: Weiwei Wang: None

Background: Medulloblastoma (MB) is one of the most common malignant tumors of the central nervous system in children, it was shown to consist of four molecular subgroups (WNT, SHH, Group 3 and Group 4). However, there is a lack of studies focusing on MB based on the four molecular subgroups in the Chinese population. To our knowledge, this is the first report systematically investigating the clinical characteristics and prognosis of the four molecular subgroups of MB in a large Chinese cohort.

Design: A total of 183 patients with MB were enrolled in the study. A nanoString-based multigene assay was undertaken to test the four molecular subgroups. Kaplan-Meier method was used to calculate survival curves of progression free survival (PFS) and overall survival (OS). A chi-square test was used to compare the proportions/frequencies between the molecular subgroups. The comparison of survival rates in different groups was conducted by the Log-rank test. To correct for multiple comparisons, a Bonferroni adjusted *p* value was used as significance threshold in these analyses. Multivariate analysis was used to evaluate independent prognostic factors.

Results: 183 MBs were classified into four molecular subgroups by nanoString assay: WNT subgroup (28 cases), SHH subgroups (33 cases), Group 3 (80 cases) and Group 4 (42 cases). The WNT subgroup predicted better prognosis than Group 3 (PFS, p=0.001, OS, p=0.002) and Group 4 (PFS, p=0.002, OS, p=0.004). Also, the prognosis of SHH subgroup was better than that of Group 3 (PFS, p=0.001, OS, p=0.010) and Group 4 (PFS, p=0.008, OS, p=0.015). In multivariate analysis, the molecular subgroups were the independent prognostic factors in patients with MB (PFS, p=0.015, OS, p=0.040).

Figure 1 - 1737

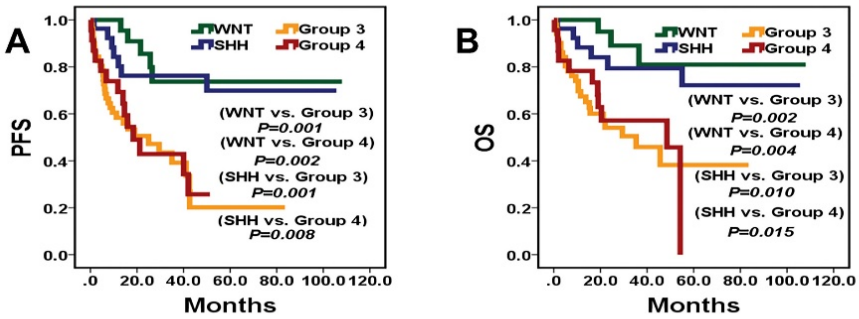

Figure 2 - 1737

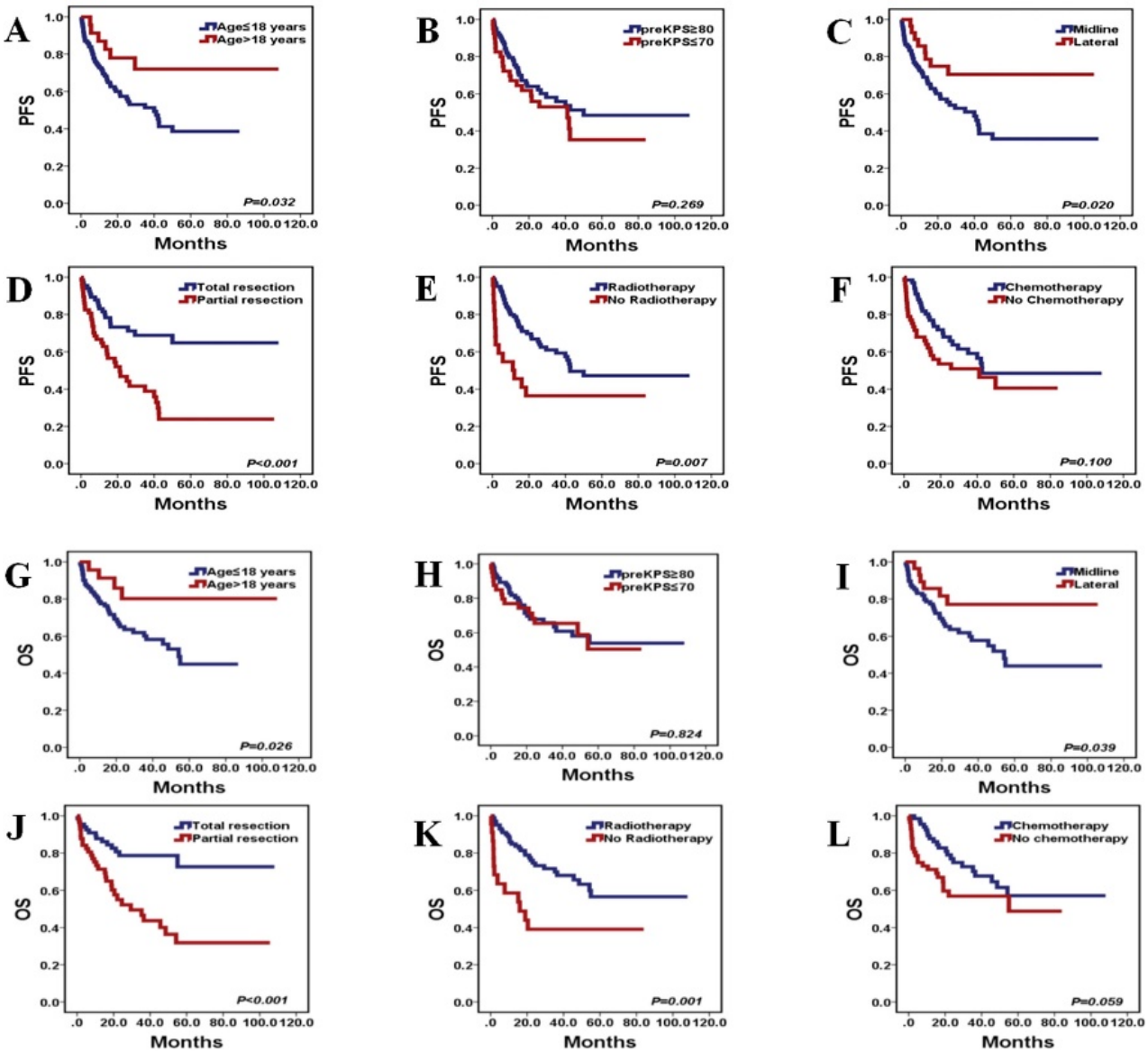

Conclusions: There exists several differences in the clinical features of the molecular subgroups of MB. The prognosis of WNT and SHH subgroup were better than those of Group 3 and Group 4. The molecular subgroup is an independent prognostic factor in Chinese patients with MB.

1738 The Smallest 14q Deletion Reported so Far in Relapsed Patients with 1p/19q Co-Deleted Oligodendrogliomas, Narrowing Down to Two Potential Relapse-Related Genes: SEL1L and STON2

Tao Zhang[1], Miguel Guzman[2], Jacqueline Batanian[3]
[1]University of Missouri School of Medicine, Columbia, MO, [2]Saint Louis University, St. Louis, MO, [3]SLU, St. Louis, MO

Disclosures: Tao Zhang: None; Miguel Guzman: None; Jacqueline Batanian: None

Background: Patients with 1p/19q co-deleted oligodendrogliomas are well known to have good respond to chemotherapy and radiation therapy, however, disease progression or recurrence is a common complication of these tumors. Published data show that loss of 14q is common in higher grade oligodendrogliomas and related to poor progression. Currently, the gene responsible for the disease relapse remains unknown. Our patient who was presented with a 1p/19q co-deleted oligodendroglioma in 2013 relapsed in 2019 showing additional abnormalities including 14q deletion. By array -comparative genome hybridization (a-CGH) method of our patient deletion and extensive literature review of all 14q a-CGH deletions found in relapsed/advanced oligodendrogliomas patients, we are reporting on the smallest 14q deletion that encompasses two potential relapse-related genes in patients with 1p/19q co-deleted oligodendrogliomas.

Design: We compared genomic coordinations if available and cytogenetic bands of our patient with 12 of published cases of 14q deletions found in patients with1p/19q co-deleted oligodendrogliomas. By excluding two 14q regions published to be not significant in relapsed 1p/19q co-deletion patients, our patient smallest 14q deletion narrows down the critical region to 14q31.1-31.2 cytogenetics bands.

Results: The critical identified region 14q31.1-31.2 encompasses six genes: NRXN3, DIO2, TSHR, GTF2A1, STON2 and SEL1L. Among which, two excellent biological genes: the SEL1L gene and the STON2 gene, are significant genes already reported in several types of cancer. In particularly, the SEL1L gene was recently found to play a role in malignant gliomas .

Conclusions: By excluding already-reported non-significant 14q region losses, the current identified smallest 14q deletion allowed us to narrow down the region to 14q31.1-31.2 that encompassed two cancer genes: SEL1L that is differentially expressed in variety of tumors including brain tumors and normal tissues and play a role in tumor growth and aggressiveness and, STON2 that is relatively less studied in tumors except ovarian cancer. Our study suggests that SEL1L and STON2 may play a role in disease relapse in patients with in recurrent 1p/19q co-deleted oligodendrogliomas suggesting future gene-target therapies.